JPET Fast Forward. Published on February 22, 2012 as DOI: 10.1124/jpet.111.188714
This article has not been copyedited and formatted. The final version may differ from this version.
JPET #188714

Binding Kinetics Redefine the Antagonist Pharmacology of the Corticotropin Releasing Factor Type 1 Receptor

Beth A. Fleck*, Sam R.J. Hoare*, Rebecca R. Pick, Margaret M. Bradbury, and Dimitri E. Grigoriadis

Neurocrine Biosciences Inc., California.

Running title: CRF_1 receptor binding kinetics

Corresponding author:

Samuel R.J. Hoare,

Neurocrine Biosciences Inc.,

12780 El Camino Real,

San Diego, CA 92130

USA

Tel: 858 617 7678

Fax: 858 617 7601

email: shoare@neurocrine.com

number of text pages – 58

number of tables – 3

number of figures – 9

number of references – 40

number of words in abstract – 250

number of words in Introduction – 719

number of words in Discussion – 1430

Recommended Section: Drug Discovery and Translational Medicine

Abbreviations:

ACTH, adrenocorticotropin

antalarmin, N-butyl-N-ethyl-2,5,6-trimethyl-7-(2,4,6-trimethylphenyl)-7H-pyrrolo[2,3-d]pyrimidin-4-amine

CP-311,316, 3,6-dimethyl-4-(pentan-3-yloxy)-2-(2,4,6-trimethylphenoxy)pyridine

CRF, corticotropin releasing factor

DMP696, 8-(2,4-dichlorophenyl)-N,N-bis(methoxymethyl)-2,7-dimethylpyrazolo[1,5-a][1,3,5]triazin-4-amine

DMP904, 3-(4-methoxy-2-methylphenyl)-2,5-dimethyl-N-(pentan-3-yl)pyrazolo[1,5-a]pyrimidin-7-amine

GPCR, G-protein-coupled receptor

NBI 27914, 5-chloro-4-N-(cyclopropylmethyl)-2-methyl-4-N-propyl-6-N-(2,4,6-trichlorophenyl)pyrimidine-4,6-diamine

NBI 30775, 5-[7-(dipropylamino)-2,5-dimethylpyrazolo[1,5-a]pyrimidin-3-yl]-N,N,4-trimethylpyridin-2-amine

NBI 34041, 3-(2,4-dichlorophenyl)-9-(heptan-4-yl)-6-methyl- 1,2,5,9-tetraazatricyclo[6.3.1.$0^{4,12}$]dodeca- 2,4(12),5,7-tetraene

NBI 34416, 3-(2,4-dichlorophenyl)-6-methyl-9-(nonan-5-yl)- 1,2,5,9-tetraazatricyclo[6.3.1.$0^{4,12}$]dodeca- 2,4(12),5,7-tetraene

NBI 34417, 3-(2,4-dichlorophenyl)-6-methyl-9-(pentan-3-yl)- 1,2,5,9-tetraazatricyclo[6.3.1.$0^{4,12}$]dodeca- 2,4(12),5,7-tetraene

JPET Fast Forward. Published on February 22, 2012 as DOI: 10.1124/jpet.111.188714
This article has not been copyedited and formatted. The final version may differ from this version.

NBI 34802, Name = 9-cyclohexyl-3-(2,4-dichlorophenyl)-6-methyl- 1,2,5,9-tetraazatricyclo[6.3.1.$0^{4,12}$]dodeca- 2,4(12),5,7-tetraene

NBI 35965, (10S)-9-(cyclopropylmethyl)-3-(2,4-dichlorophenyl)- 10-ethyl-6-methyl-1,2,5,9- tetraazatricyclo[6.3.1.$0^{4,12}$]dodeca-2,4(12),5,7- tetraene

NBI 37606, (10S)-3-(2-chloro-4-fluorophenyl)-9-(cyclopropylmethyl)-10-ethyl-6-methyl-1,2,5,9- tetraazatricyclo[6.3.1.$0^{4,12}$]dodeca-2,4,6,8(12)-tetraene

NBI 37608, (10S)-9-(cyclopropylmethyl)-10-ethyl-3-(4- fluorophenyl)-6-methyl-1,2,5,9-tetraazatricyclo[6.3.1.$0^{4,12}$]dodeca-2,4,6,8(12)- tetraene

NBI 46200, 5-(4-chloro-2-methoxyphenyl)-N-[(1S)-1-(4-fluorophenyl)pentyl]-1-methyl-N-propyl-1H-1,2,4-triazol-3-amine

NBI 49721, 3-(2,4-dichlorophenyl)-9-(heptan-4-yl)-1,2,5,9-tetraazatricyclo[6.3.1.$0^{4,12}$]dodeca-2,4,6,8(12)- tetraene

NBI 78194, 3-(2,4-dichlorophenyl)-6-methyl-9-(propan-2-yl)-1,2,5,9-tetraazatricyclo[6.3.1.$0^{4,12}$]dodeca- 2,4,6,8(12)-tetraene

ONO-2333Ms, 10-(2-chloro-4-methoxyphenyl)-11-methyl-N-(pentan-3- yl)-1,8,12-triazatricyclo[7.3.0.$0^{3,7}$]dodeca- 2,7,9,11-tetraen-2-amine

pexacerfont, N-[(2R)-butan-2-yl]-8-(6-methoxy-2-methylpyridin-3-yl)-2,7-dimethylpyrazolo[1,5-a][1,3,5]triazin-4-amine

SSR125543A, 4-(2-chloro-4-methoxy-5-methylphenyl)-N-[(1S)-2-cyclopropyl-1-(3-fluoro-4-methylphenyl)ethyl]-5-methyl-N-(prop-2-yn-1-yl)-1,3-thiazol-2-amine

JPET Fast Forward. Published on February 22, 2012 as DOI: 10.1124/jpet.111.188714
This article has not been copyedited and formatted. The final version may differ from this version.

Abstract

Corticotropin releasing factor (CRF) receptor antagonists are under preclinical and clinical investigation for stress-related disorders. In this study the impact of receptor-ligand binding kinetics on CRF_1 receptor antagonist pharmacology was investigated by measuring the association rate constant (k_1), dissociation rate constant (k_{-1}) and kinetically-derived affinity at 37°C. Three aspects of antagonist pharmacology were re-evaluated: comparative binding activity of advanced compounds; *in vivo* efficacy; and structure-activity relationships. Twelve lead compounds, with little previously-noted difference of affinity, varied substantially in their kinetic binding activity, with a 510-fold range of kinetically-derived affinity (k_{-1} / k_1), 170-fold range of k_{-1} and 13-fold range of k_1. The k_{-1} values indicated previous affinity measurements were not close to equilibrium, resulting in compression of the measured affinity range. Dissociation was exceptionally slow for three ligands (k_{-1} $t_{1/2}$ of 1.6-7.2 hr at 37˚C). Differences of binding behavior were consistent with *in vivo* pharmacodynamics (suppression of adrenocorticotropin in adrenalectomized rats). Ligand concentration-effect relationships correlated with their kinetically-derived affinity. Two ligands that dissociated slowly (53 and 130 min) produced prolonged suppression, whereas only transient suppression was observed using a more rapidly-dissociating ligand (16 min). Investigating the structure-activity relationship indicated exceptionally low values of k_1, approaching 100,000-fold less than the diffusion-limited rate. Retrospective interpretation of medicinal chemistry indicates optimizing specific elements of chemical structure overcame kinetic barriers in the association pathway, for example, constraint of the pendant aromatic orthogonal to the ligand core. Collectively, these findings demonstrate receptor binding kinetics provide new dimensions for understanding and potentially advancing the pharmacology of CRF_1 receptor antagonists.

Introduction

Physiological responses to stressful stimuli are mediated by corticotropin releasing factor (CRF), a 41 amino-acid peptide that acts on the pituitary to regulate the hypothalamic-pituitary axis and the central nervous system to modulate behavioral responses to stress (Bale and Vale, 2004). CRF activates the CRF_1 receptor, a Class B G-protein-coupled receptor (GPCR) (Bale and Vale, 2004; Grigoriadis, 2005). Pathophysiological conditions can arise from dysregulation of the stress axis, including depression, post-traumatic stress disorder and relapse in substance abuse. Consequently, CRF has received considerable attention in drug discovery for psychiatric disease. The search for tractable new mechanisms for depression treatment, beyond monoamine modulators, is stimulated by the fact that existing drugs do not work effectively in approximately 30% of patients (Grigoriadis, 2005).

Antagonism of the CRF_1 receptor has been proposed for rebalancing a dysfunctional stress axis (Holsboer, 2000; Grigoriadis, 2005). Successful development of drug-like small molecule antagonists of the CRF_1 receptor (Fig. 1) required application of advanced pharmacology technology. Low-affinity lead compounds were identified in one of the early successes of high-throughput screening (Hodge et al., 1999). Screening was required because CRF is too large and complex to be used as a chemical starting point for small molecule medicinal chemistry. The compounds are allosteric modulators of the CRF_1 receptor (Hoare et al., 2003); allosteric inhibition solved the molecular weight problem, enabling a small molecule to inhibit binding of a peptide ten times its size. CRF_1 receptor antagonists were some of the first allosteric GPCR ligands to be tested clinically. In the first report of behavioral effects in humans, 5-[7-(dipropylamino)-2,5-

JPET Fast Forward. Published on February 22, 2012 as DOI: 10.1124/jpet.111.188714
This article has not been copyedited and formatted. The final version may differ from this version.

dimethylpyrazolo[1,5-a]pyrimidin-3-yl]-N,N,4-trimethylpyridin-2-amine (NBI 30775, Fig. 1) significantly reduced Hamilton depression and anxiety scores in a small group of patients with exceptionally high baseline scores (Zobel et al., 2000). In larger trials, 3,6-dimethyl-4-(pentan-3-yloxy)-2-(2,4,6-trimethylphenoxy)pyridine (CP-316,311, Fig. 1) failed to demonstrate efficacy in the treatment of major depression (Binneman et al., 2008) and pexacerfont, N-[(2R)-butan-2-yl]-8-(6-methoxy-2-methylpyridin-3-yl)-2,7-dimethylpyrazolo[1,5-a][1,3,5]triazin-4-amine (pexacerfont, Fig. 1) did not demonstrate efficacy compared to placebo for the treatment of generalized anxiety disorder (Coric et al., 2010).

Ideally, a compound with the highest possible efficacy for antagonizing the CRF_1 receptor would provide the best tool for testing the utility of this mechanism for treating psychiatric disorders. Designing receptor-ligand interactions to optimize therapeutic outcome might now be possible because of an explosion in our knowledge of and ability to measure receptor-ligand interactions and the subsequent modulation of receptor and cellular activity (see Kenakin, 2007 and accompanying reviews). A simple strategy for maximizing antagonist efficacy is to maximize receptor residence time, by slowing antagonist dissociation from the receptor (Copeland et al., 2006; Vauquelin and Van Liefde, 2006; Brinkerhoff et al., 2008; Tummino and Copeland, 2008). This strategy requires an understanding of the kinetics of receptor-ligand interaction, which has been evolving since the 1960's (Paton, 1966 ; Rocha e, 1969). With respect to GPCRs, antagonists of the angiotensin II AT_1 receptor exemplify the potential of slow dissociation to increase antagonist effect (Verheijen et al., 2004). The slowly-dissociating antagonist candesartan produces a greater maximal antihypertensive effect than more-

rapidly dissociating antagonists such as losartan (Hansson, 2001). Candesartan also produces a longer duration of effect (Lacourciere and Asmar, 1999). Ligand binding kinetics on other GPCRs are being extensively investigated, including the H1 histamine receptor, for which binding kinetics have been interpreted in the context of receptor structure and changes of Gibbs free energy (Wittmann et al., 2011); the M3 muscarinic acetylcholine receptor, for which antagonist binding has been re-evaluated kinetically (Dowling and Charlton, 2006) and agonist dissociation rate correlated with intrinsic activity (Sykes et al., 2009); and the μ-opioid receptor, for which slow buprenorphine dissociation contributes to the pharmacodynamics of the drug in humans (Yassen et al., 2006). Small molecule binding kinetics are now being measured on the CRF_1 receptor. In a recent report, residence time was shown to be the primary determinant of insurmountable antagonism *in vitro* and CRF_1 receptor binding *in vivo* (Ramsey et al., 2011). Pharmacological screening methods have been described for optimizing the dissociation rate constant (Miller et al., 2011; Ramsey et al., 2011).

In this study, we first measured the association and dissociation rate constants of small molecule binding to the CRF_1 receptor. We discovered the kinetics of binding differed substantially between lead molecules and that association and dissociation were remarkably slow. We then investigated the extent to which the binding kinetics rationalize pharmacokinetic differences and structure-activity relationships.

JPET Fast Forward. Published on February 22, 2012 as DOI: 10.1124/jpet.111.188714
This article has not been copyedited and formatted. The final version may differ from this version.

Materials and Methods

Materials – The following compounds were synthesized using published methods (see the following reviews for original references: Gilligan et al., 2000b; Kehne and De Lombaert, 2002; Gross et al., 2005; Li et al., 2005; Zorrilla and Koob, 2010).

5-chloro-4-N-(cyclopropylmethyl)-2-methyl-4-N-propyl-6-N-(2,4,6-trichlorophenyl)pyrimidine-4,6-diamine (NBI 27914)

N-butyl-N-ethyl-2,5,6-trimethyl-7-(2,4,6-trimethylphenyl)-7H-pyrrolo[2,3-d]pyrimidin-4-amine (antalarmin)

3,6-dimethyl-4-(pentan-3-yloxy)-2-(2,4,6-trimethylphenoxy)pyridine (CP-316,311)

8-(2,4-dichlorophenyl)-N,N-bis(methoxymethyl)-2,7-dimethylpyrazolo[1,5-a][1,3,5]triazin-4-amine (DMP696)

3-(4-methoxy-2-methylphenyl)-2,5-dimethyl-N-(pentan-3-yl)pyrazolo[1,5-a]pyrimidin-7-amine (DMP904)

5-[7-(dipropylamino)-2,5-dimethylpyrazolo[1,5-a]pyrimidin-3-yl]-N,N,4-trimethylpyridin-2-amine (NBI 30775)

3-(2,4-dichlorophenyl)-9-(heptan-4-yl)-6-methyl-1,2,5,9-tetraazatricyclo[6.3.1.$0^{4,12}$]dodeca- 2,4(12),5,7-tetraene (NBI 34041)

(10S)-9-(cyclopropylmethyl)-3-(2,4-dichlorophenyl)- 10-ethyl-6-methyl-1,2,5,9-tetraazatricyclo[6.3.1.$0^{4,12}$]dodeca-2,4(12),5,7- tetraene (NBI 35965)

5-(4-chloro-2-methoxyphenyl)-N-[(1S)-1-(4-fluorophenyl)pentyl]-1-methyl-N-propyl-1H-1,2,4-triazol-3-amine (NBI 46200)

JPET Fast Forward. Published on February 22, 2012 as DOI: 10.1124/jpet.111.188714
This article has not been copyedited and formatted. The final version may differ from this version.

10-(2-chloro-4-methoxyphenyl)-11-methyl-N-(pentan-3-yl)-1,8,12-triazatricyclo[7.3.0.0^{3,7}]dodeca- 2,7,9,11-tetraen-2-amine (ONO-2333Ms)

N-[(2R)-butan-2-yl]-8-(6-methoxy-2-methylpyridin-3-yl)-2,7-dimethylpyrazolo[1,5-a][1,3,5]triazin-4-amine (pexacerfont)

4-(2-chloro-4-methoxy-5-methylphenyl)-N-[(1S)-2-cyclopropyl-1-(3-fluoro-4-methylphenyl)ethyl]-5-methyl-N-(prop-2-yn-1-yl)-1,3-thiazol-2-amine (SSR125543A).

Analogues of NBI 35965 and NBI 34041 all described in (Gross et al., 2005):

3-(2,4-dichlorophenyl)-6-methyl-9-(nonan-5-yl)-1,2,5,9-tetraazatricyclo[6.3.1.0^{4,12}]dodeca- 2,4(12),5,7-tetraene (NBI 34416)

3-(2,4-dichlorophenyl)-6-methyl-9-(pentan-3-yl)-1,2,5,9-tetraazatricyclo[6.3.1.0^{4,12}]dodeca- 2,4(12),5,7-tetraene (NBI 34417)

9-cyclohexyl-3-(2,4-dichlorophenyl)-6-methyl-1,2,5,9-tetraazatricyclo[6.3.1.0^{4,12}]dodeca- 2,4(12),5,7-tetraene (NBI 34802)

(10S)-3-(2-chloro-4-fluorophenyl)-9-(cyclopropylmethyl)-10-ethyl-6-methyl-1,2,5,9- tetraazatricyclo[6.3.1.0^{4,12}]dodeca-2,4,6,8(12)-tetraene (NBI 37606)

(10S)-9-(cyclopropylmethyl)-10-ethyl-3-(4-fluorophenyl)-6-methyl-1,2,5,9-tetraazatricyclo[6.3.1.0^{4,12}]dodeca-2,4,6,8(12)- tetraene (NBI 37608)

3-(2,4-dichlorophenyl)-9-(heptan-4-yl)-1,2,5,9-tetraazatricyclo[6.3.1.0^{4,12}]dodeca-2,4,6,8(12)- tetraene (NBI 49721)

3-(2,4-dichlorophenyl)-6-methyl-9-(propan-2-yl)-1,2,5,9-tetraazatricyclo[6.3.1.0^{4,12}]dodeca- 2,4,6,8(12)-tetraene (NBI 78194)

[^{3}H]NBI 35965 was prepared as described previously (Gross et al., 2005). [^{3}H]NBI 30775 was prepared using the same method, using the 6-bromo pyrazolopyrimidine intermediate. ^{125}I-[Tyr^{0}]sauvagine was from PerkinElmer (Waltham, MA). Dulbecco's phosphate-buffered saline (DPBS) and cell culture supplies were from

JPET Fast Forward. Published on February 22, 2012 as DOI: 10.1124/jpet.111.188714
This article has not been copyedited and formatted. The final version may differ from this version.

Invitrogen (Carlsbad, CA). Fetal bovine serum was from HyClone (Logan, UT). All other reagents were from Sigma-Aldrich (St. Louis, MO). Low-binding 96-well plates (#3605) were from Corning (Palo Alto, CA). Unifilter GF/C plates and Microscint 20 scintillation fluid were from PerkinElmer (Boston, MA).

Radioligand binding assays conditions – Binding experiments were performed in low binding 96-well plates in assay buffer, comprised of DPBS (1.5 mM KH_2PO_4, 8.1 mM Na_2HPO_4, 2.7 mM KCl, 138 mM NaCl), supplemented with 10 mM $MgCl_2$, 2 mM ethylene glycol-bis[β-aminoethyl]-N,N,N',N'-tetraacetic acid, set to pH 7.4 with NaOH. All binding assays employing [^{3}H]NBI 35965 or [^{3}H]NBI 30775 included 10 μM GTPγS to uncouple receptor from G-protein, and protease inhibitors (1:1000 dilution of protease inhibitor cocktail P8340 from Sigma–Aldrich, final assay concentrations of 0.1 mM 4-(2-aminoethyl)benzenesulfonyl fluoride hydrochloride, 850 nM aprotonin, 422 μM bestatin hydrochloride, 1.4 μM N-(trans-epoxysuccinyl)-L-leucine 4- guanidinobutylamide, 1.9 μM leupeptin hemisulfate and 1.53 μM pepstatin A). Nonspecific binding in every experiment was defined by addition of 4 μM NBI 34041. (All compound concentrations listed within represent final concentrations in the assay.) Specific binding for each concentration of radioligand at each time point was determined by subtracting nonspecific binding from total binding. The cell membranes used were isolated from HEK293 Flp-In cells (Invitrogen, Carlsbad, CA) stably expressing the CRF_1 receptor at 62 pmol/mg membrane protein (Hoare et al., 2004). Membranes were isolated by high-pressure nitrogen cavitation and differential centrifugation as described previously (Hoare et al., 2003). The assay mixture (total volume of 200 μl) was incubated for times

and temperatures indicated on a temperature-controlled reaction block designed to fit 16 round-bottom 96-well plates used (J-KEM, St. Louis, MO, see http://www.jkem.com/crbhof.html). At the end of the incubation period bound and free radioligand were separated by rapid vacuum filtration onto Unifilter GF/C filter plates. GF/C filter plates were pretreated with 0.5% polyethylenimine in distilled water for 30 min and were pre-rinsed with 200 µl per well 1% bovine serum albumin in DPBS immediately before harvesting of the assay plate using a cell harvester (UniFilter-96 Filtermate; PerkinElmer). Filters were then washed two times with 400 µl DPBS. Filter plates were dried, 50 µl Microscint 20 added and the plate was monitored for radioactivity using a TopCount NXT (PerkinElmer) at 30% efficiency. The total amount of radioligand added to the assay was measured using a 1600TR liquid scintillation counter (PerkinElmer) at 47% efficiency.

Radioligand dissociation assays – Radioligand dissociation experiments were performed by pre-incubating cell membranes with radioligand for 2 hr. The target concentration of radioligand, temperature, amount of membrane protein and dissociation time period employed were: 10 nM [^{3}H]NBI 35965 at 22 °C, 4 µg membrane protein and 5 hr; 10 nM [^{3}H]NBI 30775 at 22 °C, 9.5 µg membrane protein and 5 hr; 3 nM [^{3}H]NBI 35965 at 37ºC, 5 µg membrane protein and 7 hr; and 3 nM [^{3}H]NBI 30775 at 37 °C, 5 µg membrane protein and 7 hr. Dissociation was initiated by the addition of 4 µM NBI 34041. Bound radioligand was harvested at twelve time points using the method described above. Non-specific binding was measured by including 4 µM NBI 34041 in the pre-incubation phase of the experiment. In each experiment, one duplicate set of wells

JPET Fast Forward. Published on February 22, 2012 as DOI: 10.1124/jpet.111.188714
This article has not been copyedited and formatted. The final version may differ from this version.

did not receive unlabeled compound in the dissociation phase of the experiment in order to measure the stability of total radioligand binding over time. Total radioligand binding remained stable over the time period measured (5 hr at 22 °C and 7 hr 37ºC, data not shown).

Radioligand association assays – Radioligand association experiments were initiated by the addition of cell membranes to wells containing radioligand. For [^{3}H]NBI 35965 at 22 °C, 6 concentrations were tested ranging from 450 pM - 20 nM (n=3) using 4 μg membrane protein, and at 37ºC a single concentration of approximately 3 nM (n=2) was tested. For [^{3}H]NBI 30775 at 22 °C, 6 concentrations were tested ranging from 1 nM - 20 nM (n=3) using 8 μg membrane protein, and at 37ºC, a single concentration of approximately 3 nM (n=2) was tested. For all assays at 37°C, before addition of membrane, plates and membrane solution were warmed to 37° using the heat block and a water bath, respectively. Bound radioligand was harvested as described above at twelve time points between 2 min and 2.5 hr. The association experiments to determine the receptor kinetic rate constants of the unlabeled ligands were performed in the same manner using approximately 3 nM [^{3}H]NBI 30775, either in the absence or in the presence of a range of a range of concentrations of unlabeled ligand. For lead compounds (Table 1), four or five concentrations of unlabeled ligand and fifteen time points were used (ranging from 60 seconds to 4 hr). For kinetic SAR (Figs. 5-8), two concentrations of unlabeled ligand and sixteen time points were used (ranging from 20 seconds to 4 hr).

JPET Fast Forward. Published on February 22, 2012 as DOI: 10.1124/jpet.111.188714
This article has not been copyedited and formatted. The final version may differ from this version.

Competition binding assays – Unlabeled ligands were competed against ^{125}I-sauvagine, in the absence of GTPγS, or [^{3}H]NBI 35965, in the presence of 10 μM GTPγS, at 22 °C for 2 hr. Twelve concentrations of unlabeled ligand were tested, ranging from 10 μM to 31.6 pM by 3.16-fold serial dilution. The concentration of radioligand varied from 63-110 pM for ^{125}I-sauvagine and 1.3-1.8 nM for [^{3}H]NBI 35965. The amount of membrane protein in the assay was 2 μg per well for both radioligands.

Measurement of adrenocorticotropin in adrenalectomized rats – All animal studies were approved by the Institutional Animal Care and Use Committee at Neurocrine Biosciences. Rats were received at 175-200g from Charles River Laboratories (San Diego, CA) and housed in a 12 hr-12 hr light cycle for one week prior to adrenalectomy. Rats were anesthetized with isoflurane and the whole adrenal capsule was plucked out of the intraperitoneal cavity. All external incisions were closed using wound clips. The ability of adrenalectomized animals to maintain normal electrolyte levels is compromised, fat metabolism is altered and glucose storage impaired. Thus, water containing 0.9% NaCl + 1.0% sucrose and regular rat chow were provided *ad libitum*. Their diet was also supplemented daily with 2 pellets of sweetened condensed milk chow (Research Diets, Inc. # D12266B) and a 3 ml subcutaneous injection of lactated Ringer solution. Adrenalectomy was verified by plasma corticosterone measurements: Seven days after surgery, blood was drawn from the tail vein and corticosterone radioimmunoassay (MP Biomedicals, Irvine, CA) was performed on the serum. Only rats with a corticosterone level below 10 ng/ml were used in the study. Seven days after adrenalectomy, rats were implanted with femoral vein catheters. Approximately four days

later, rats were prepared for blood sampling by attaching their catheters to PE50 tubing and a syringe and acclimated to individual opaque sampling cages for 2 hr. These cages allow sampling to occur without disturbance to the rat. After a baseline blood sample (0.3 ml), rats received intravenous injection of vehicle (10% cremaphore), or test compound in vehicle. Blood samples were taken at the time points indicated in Fig. 5. Blood volumes were replaced with 5 U/ml heparinized saline. Blood samples were stored on ice with ethylenediaminetetraacetic acid and plasma separated by centrifugation at 4°C and then stored at –80°C for subsequent measurement of adrenocorticotropin (ACTH) by radioimmunoassay (MP Biomedicals, Irvine, CA). The plasma compound concentration in these blood samples was measured as follows. Proteins in plasma samples were precipitated with 200 µL of acetonitrile, after adding 25-50 µL of internal standard. The organic layer was then isolated by centrifugation and dried. Afterward reconstitution with 30/70/0.1% acetonitrile / water / formic Acid, the material was introduced into a SCIEX API-3000 LC-MS-MS system for analysis (ESPI+) (Danaher Corp. Washington, DC).

Data and statistical analysis – All data were analyzed using Prism 4.0 (GraphPad Software, La Jolla, CA). Radioligand dissociation data (specific binding) were fit to monophasic and biphasic association equations, with the plateau of the specific binding set to zero, and the best fit determined using a partial F-test. A monophasic model (eq. 1) fit best in all cases ($p > 0.05$).

$$Y = Y_{t=0}e^{-k_{-1(L)}t} \quad \text{eq. 1}$$

$k_{-1(L)}$ is the radioligand dissociation rate constant, t is time in min, $Y_{t=0}$ is specific binding at the initiation of the dissociation phase of the assay. Radioligand association binding

JPET Fast Forward. Published on February 22, 2012 as DOI: 10.1124/jpet.111.188714
This article has not been copyedited and formatted. The final version may differ from this version.

data (specific binding) were fit to monophasic and biphasic association equations and the best fit determined using a partial F-test. A monophasic model (eq. 2) fit best for all experiments ($p > 0.05$).

$$Y = Y_{max}(1 - e^{-k_{obs}t}) \quad \text{eq. 2}$$

where t is time in min, k_{obs} is the observed association rate constant, Y is specific binding at time t, and Y_{max} is specific binding at infinite t. To determine the radioligand association rate constant tested at 22 °C, where multiple concentrations of radioligand were used, k_{obs} was plotted against the radioligand concentration, and the data analyzed by linear regression using eq. 3:

$$k_{obs} = [L]k_{1(L)} + k_{-1(L)} \quad \text{eq. 3}$$

where $k_{1(L)}$ is the radioligand association rate constant and [L] is the radioligand concentration. The fitted value of the slope yields $k_{1(L)}$. The Y intercept ($k_{-1(L)}$) was fixed at the mean $k_{-1(L)}$ value measured from radioligand dissociation experiments (Table 1). To determine the radioligand association rate constant at 37ºC where a single concentration of radioligand was tested, eq. 4 was used, with $k_{-1(L)}$ set to its directly measured value from the dissociation experiments:

$$k_{1(L)} = \frac{k_{obs} - k_{-1(L)}}{[L]} \quad \text{eq. 4}$$

The association and dissociation rate constants of unlabeled ligands were measured using the method of Motulsky and Mahan in which association of a labeled radioligand is

JPET Fast Forward. Published on February 22, 2012 as DOI: 10.1124/jpet.111.188714
This article has not been copyedited and formatted. The final version may differ from this version.

measured in the absence and presence of the unlabeled test ligand (Motulsky and Mahan, 1984). The analysis assumes the model in Scheme 1:

$$RL \underset{k_{-1(L)}}{\overset{k_{1(L)}}{\rightleftharpoons}} R + L + I \underset{k_{-1(I)}}{\overset{k_{1(I)}}{\rightleftharpoons}} RI$$

Scheme 1

R is the receptor, L is the radioligand, $k_{1(L)}$ is the radioligand association rate constant, $k_{-1(L)}$ is the radioligand dissociation rate constant, I is the unlabeled ligand, $k_{1(I)}$ is the unlabeled ligand association rate constant and $k_{-1(I)}$ is the unlabeled ligand dissociation rate constant. Kinetic constants for the unlabeled ligands were determined by measuring the time course of association of [^{3}H]NBI 30775 in the absence of unlabeled ligand and in the presence of a range of unlabeled ligand concentrations. Specific radioligand binding (RL) was globally fit to a two-component exponential curve by non-linear regression using the 'Kinetics of competitive binding' equation provided in Prism 4.0:

$$Y = Q\left(\frac{k_{-1(I)}(K_F - K_S)}{K_F K_S} + \frac{k_{-1(I)} - K_F}{K_F} e^{-K_F X} - \frac{k_{-1(I)} - K_S}{K_S} e^{-K_S X}\right) \quad \text{eq. 5}$$

JPET Fast Forward. Published on February 22, 2012 as DOI: 10.1124/jpet.111.188714
This article has not been copyedited and formatted. The final version may differ from this version.

$$Q = \frac{B_{max} k_{1(L)}[L]}{K_F - K_S}$$

$$K_F = 0.5(K_A + K_B + S)$$

$$K_S = 0.5(K_A + K_B - S)$$

$$S = \sqrt{(K_A - K_B)^2 + 4k_{1(L)}k_{1(I)}[L][I]}$$

$$K_A = k_{1(L)}[L] + k_{-1(L)}$$

$$K_B = k_{1(I)}[I] + k_{-1(I)}$$

where X is time (min), Y is specific radioligand binding (cpm) and B_{max} is the total amount of receptor in the assay (cpm). Radioligand association data for the control (no unlabeled ligand) and for the presence of multiple concentrations of unlabeled ligand were fitted globally to this equation (Dowling and Charlton, 2006). The globally fitted parameters were B_{max}, $k_{1(L)}$, $k_{1(I)}$, and $k_{-1(I)}$. The fixed parameters were $k_{-1(L)}$, [L] and [I]. The association rate constant of [^{3}H]NBI 30775 ($k_{1(L)}$) was fit for each experiment as an internal control, and $k_{1(L)}$ determined by the global fit closely matched the $k_{1(L)}$ value determined by direct measurement of [^{3}H]NBI 30775 association alone (Table 1). In early experiments on the lead compounds (Table 2) four or five concentrations of compound were tested in each experiment and used in the global fitting. Subsequently it was determined that fitted values with an equivalent standard error within the fit could be obtained from using two concentrations of unlabeled ligand in the experiment. Consequently most data for the kinetic SAR (Figs. 6-8) were obtained from assays

JPET Fast Forward. Published on February 22, 2012 as DOI: 10.1124/jpet.111.188714
This article has not been copyedited and formatted. The final version may differ from this version.

employing two concentrations of unlabeled ligand. The global r^2 values from the fits ranged from 0.90-0.98.

In the figures, tables and text, the association rate constant from either labeled or unlabeled ligands is denoted as k_1 and the dissociation rate constant for labeled or unlabeled ligands denoted as k_{-1}. The half-life of drug dissociation from the receptor ($t_{1/2}$), also equal to the median residence time, was calculated from the dissociation rate constant, k_{-1}, using the following equation:

$$t_{1/2} = \frac{0.693}{k_{-1}} \qquad \text{eq. 6}$$

The kinetically-derived affinity (kinetic K_d for radioligands, kinetic K_i for unlabeled ligands) was determined using eq 7:

$$K_d \text{ or } K_i = \frac{k_1}{k_{-1}} \qquad \text{eq. 7}$$

Statistical comparison of rate constant data - We compared the different groups of the structure-activity relationship data (Figs 6, 7 and 8) using one-way analysis of variance, followed by the Newman-Keuls Multiple Comparison Test to compare pairs of compounds. The results are given in the legends to Figs 6, 7 and 8. The logarithm of the k_1 value was used in the test because it was assumed to be normally-distributed. The linear value of k_{-1} has been shown to be normally distributed (Christopoulos, 1998). The log value but not the linear value of K_d (k_{-1} / k_1) is normally distributed, so it was assumed that the log value of the denominator, k_1, was normally distributed.

JPET Fast Forward. Published on February 22, 2012 as DOI: 10.1124/jpet.111.188714
This article has not been copyedited and formatted. The final version may differ from this version.

Results

Receptor binding kinetics of radiolabeled CRF_1 receptor antagonists – Numerous nonpeptide antagonists have been developed that bind with high affinity to the CRF_1 receptor but the kinetics of their interaction with the receptor have not been systematically evaluated. We measured the kinetic parameters of these ligands' interaction with the CRF_1 receptor, specifically the association rate constant, k_1, dissociation rate constant, k_{-1}, and kinetically-derived affinity (K_d or K_i, equal to k_{-1} / k_1). We first examined the tritiated form of (10S)-9-(cyclopropylmethyl)-3-(2,4-dichlorophenyl)-10-ethyl-6-methyl-1,2,5,9-tetraazatricyclo[6.3.1.$0^{4,12}$]dodeca-2,4(12),5,7-tetraene ([^{3}H]NBI 35965) and [^{3}H]NBI 30775 (Fig. 1). The kinetics of binding were consistent with a single-site binding interaction with the CRF_1 receptor; time-course data were fit best by mono-exponential rate equations (Fig. 2) and the dependence of the observed association rate on radioligand concentration was linear up to 45 nM [^{3}H]NBI 35965 and 20 nM [^{3}H]NBI 30775 (data not shown). At 22°C, a temperature commonly used in CRF_1 receptor binding assays, radioligand dissociation was markedly slow (Fig. 2A, Table 1). For [^{3}H]NBI 35965 k_{-1} was 0.0023 min^{-1} (median residence time, or k_{-1} $t_{1/2}$, of 5 hr). [^{3}H]NBI 30775 dissociated too slowly to enable accurate measurement of k_{-1} as receptor occupancy had decreased by only 10% after 5 hr (Fig. 2A). A similarly slow rate of dissociation of NBI 30775 at room temperature has been reported (Ramsey et al., 2011) and slow antagonist dissociation at room temperature has been observed for numerous GPCRs (Anthes et al., 2002; Fierens et al., 2002; Dowling and Charlton, 2006; Tummino and Copeland, 2008). In an attempt to better define the dissociation rate constant, the assay temperature was increased to 37°C.

JPET Fast Forward. Published on February 22, 2012 as DOI: 10.1124/jpet.111.188714
This article has not been copyedited and formatted. The final version may differ from this version.

This increase markedly accelerated radioligand dissociation; the residence time of [^{3}H]NBI 35965 decreased from 5 hr to 17 min (Fig. 2A, Table 1). Dissociation of [^{3}H]NBI 30775 was accelerated to a slow but measurable rate (k_{-1} $t_{1/2}$ of 3.2 hr, Fig. 2A, Table 1). A similar magnitude of k_{-1} increase was also observed for [^{3}H]candesartan on the AT_1 receptor (Fierens et al., 2002). Raising the incubation temperature to 37°C also accelerated radioligand association, 5.5-fold to 22 $10^6M^{-1}min^{-1}$ for [^{3}H]NBI 35965 and 2.8-fold to 31 $10^6M^{-1}min^{-1}$ for [^{3}H]NBI 30775 (Fig. 2B, Table 1). These rates of ligand association and dissociation at 37°C were unusually slow compared with antagonists of other GPCRs. The k_1 values of 22 and 31 $10^6M^{-1}min^{-1}$ are much less than the diffusion-limited rate constant [approximately 10,000 $10^6M^{-1}min^{-1}$ (Copeland et al., 2006)]. These k_1 values are also less than values reported for several antagonists of Class A GPCRs, in the range of 1,000 $10^6M^{-1}min^{-1}$ (see references cited in Tummino and Copeland, 2008). In addition dissociation of [^{3}H]NBI 30775 from the CRF_1 receptor was exceptionally slow, even at 37°C ($t_{1/2}$ of 3.2 hr).

Binding kinetics of high-affinity unlabeled CRF_1 receptor antagonists – Slow antagonist dissociation can contribute to maximizing the duration and possibly the extent of *in vivo* efficacy of antagonist compounds (Copeland et al., 2006). Therefore we determined if other CRF_1 receptor antagonists beyond NBI 30775 dissociated slowly. In addition, slow binding kinetics can distort measurements of binding affinity (Aranyi and Quiroga, 1980; Motulsky and Mahan, 1984) owing to lack of equilibrium in the assay. [Equilibrium is approximated in competition binding assays by a time interval at least 3-fold the residence time of the slowest-dissociating ligand in the assay (Motulsky and Mahan,

JPET Fast Forward. Published on February 22, 2012 as DOI: 10.1124/jpet.111.188714
This article has not been copyedited and formatted. The final version may differ from this version.

1984)]. For the CRF_1 receptor, competition binding assays by us and other groups have typically been performed for 1-2 hr at 22°C. Under these conditions NBI 35965 and NBI 30775 binding is not even close to equilibrium; an incubation time of at least 15 hours would be required for NBI 35965 to reach equilibrium with the CRF_1 receptor at 22°C (calculated from data in Table 1). Consequently we re-evaluated the binding affinity of lead compounds using the affinity derived from kinetic measurements (k_{-1} / k_1), a method for determining binding affinity that avoids distortion of affinity measurements resulting from lack of equilibration.

We used the method of Motulsky and Mahan to measure the binding kinetic constants of the antagonists, which determines the association and dissociation rate constants of an unlabeled compound from its effect on the association rate of a radioligand (Motulsky and Mahan, 1984). Fig. 3 shows representative data for four ligands with varying k_{-1} values. For unlabeled NBI 35965 and NBI 30775 (Fig. 3B and C), the association and dissociation rate constants and kinetically-derived affinity closely matched those of the radiolabeled versions of the compounds at both 22°C and 37ºC (Table 1), validating the method. To characterize binding kinetics of other compounds (Fig. 1) we chose the physiologic assay temperature of 37°C, instead of 22°C, to accelerate dissociation into a measurable range for slowly-dissociating compounds. [^{3}H]NBI 30775 was employed as the radioligand because it provided the highest total binding : nonspecific binding ratio of the radioligands tested, and because it dissociates slowly, enabling more accurate measurement of the k_{-1} value of slowly-dissociating ligands (Motulsky and Mahan, 1984).

JPET Fast Forward. Published on February 22, 2012 as DOI: 10.1124/jpet.111.188714
This article has not been copyedited and formatted. The final version may differ from this version.

We evaluated the comparative kinetic pharmacology of twelve lead CRF_1 receptor antagonists, selected based on progression to advanced preclinical or early clinical testing (Fig. 1). Compounds tested were CP-316,311, NBI 30775, NBI 35965, pexacerfont, N-butyl-N-ethyl-2,5,6-trimethyl-7-(2,4,6-trimethylphenyl)-7H-pyrrolo[2,3-d]pyrimidin-4-amine (antalarmin), 8-(2,4-dichlorophenyl)-N,N-bis(methoxymethyl)-2,7-dimethylpyrazolo[1,5-a][1,3,5]triazin-4-amine (DMP696), 3-(4-methoxy-2-methylphenyl)-2,5-dimethyl-N-(pentan-3-yl)pyrazolo[1,5-a]pyrimidin-7-amine (DMP904), 5-chloro-4-N-(cyclopropylmethyl)-2-methyl-4-N-propyl-6-N-(2,4,6-trichlorophenyl)pyrimidine-4,6-diamine (NBI 27914), 3-(2,4-dichlorophenyl)-9-(heptan-4-yl)-6-methyl- 1,2,5,9-tetraazatricyclo[6.3.1.$0^{4,12}$]dodeca- 2,4(12),5,7-tetraene (NBI 34041), 5-(4-chloro-2-methoxyphenyl)-N-[(1S)-1-(4-fluorophenyl)pentyl]-1-methyl-N-propyl-1H-1,2,4-triazol-3-amine (NBI 46200), 10-(2-chloro-4-methoxyphenyl)-11-methyl-N-(pentan-3-yl)-1,8,12-triazatricyclo[7.3.0.$0^{3,7}$]dodeca- 2,7,9,11-tetraen-2-amine (ONO-2333Ms), and 4-(2-chloro-4-methoxy-5-methylphenyl)-N-[(1S)-2-cyclopropyl-1-(3-fluoro-4-methylphenyl)ethyl]-5-methyl-N-(prop-2-yn-1-yl)-1,3-thiazol-2-amine (SSR125543A).

Under standard *in vitro* assay conditions, competition against a radiolabeled peptide agonist at 22°C, all these ligands have been described as high affinity ligands, with little noted difference between their affinity for the CRF_1 receptor (Li et al., 2005) (see also Fig. 4A). Measuring their binding kinetics revealed considerable differences of receptor-binding activity (Fig 4, Table 2). The dissociation rate constant varied by 170-fold, from a k_{-1} $t_{1/2}$ of 2.6 min for NBI 27914 to 7.2 hr for SSR125543A (Fig. 4B, Table 2). Three ligands bound with a long residence time (k_{-1} $t_{1/2}$ of > 1 hr, DMP904, NBI

JPET Fast Forward. Published on February 22, 2012 as DOI: 10.1124/jpet.111.188714
This article has not been copyedited and formatted. The final version may differ from this version.

30775 and SSR125543A, Fig. 3C and 3D, Fig. 4B, Table 2). A long CRF_1 receptor residence time has been reported for NBI 30775 and DMP-904 at room temperature (Ramsey et al., 2011). The association rate constant varied from 2.6 $10^6M^{-1}min^{-1}$ for pexacerfont to 33 $10^6M^{-1}min^{-1}$ for SSR125543A (Table 2), values much less than the diffusion-limited rate constant [approximately 10,000 $10^6M^{-1}min^{-1}$ (Copeland et al., 2006)]. Remarkably, the kinetic K_i (k_{-1} / k_1) varied by 510-fold, from 49 pM for SSR125543A to 25 nM for NBI 27914 (Fig. 4A). This range was greater than the range of apparent affinity determined using the previously-utilized ('traditional') binding assay conditions (competition against ^{125}I-sauvagine at 22°C, 25-fold range from 0.3 nM for SSR125543A to 7.4 nM for pexacerfont, Fig. 4A, Table 3). We are currently investigating the difference of affinity further using a direct measurement of ligand binding, frontal affinity chromatography coupled to mass spectrometry (FAC-MS, Slon-Usakiewicz et al., 2005). In these experiments, membranes are immobilized using artificial phospholipids coupled to a solid support. Ligands are continuously infused and affinity measured as a function of the elution time, the ligand detected directly using mass spectrometry. In our first experiments, the affinity of DMP696 was 23 nM and NBI 30775 was 0.60 nM.

We investigated the reason for the discrepancy between the affinity range from kinetic measurements and from traditional assay conditions. This difference was not due to the different nature of the radioligands used (nonpeptide antagonist versus peptide agonist) because the apparent ligand affinity in competition against the nonpeptide antagonist [^{3}H]NBI 35965 at 22°C was not significantly different from the apparent affinity measured using ^{125}I-sauvagine (Table 3). Next, we investigated the extent to

JPET Fast Forward. Published on February 22, 2012 as DOI: 10.1124/jpet.111.188714
This article has not been copyedited and formatted. The final version may differ from this version.

which lack of equilibration at 22°C could affect the measurement of apparent affinity in a competition assay, using simulated data. We simulated inhibition of [^{3}H]NBI 35965 binding by unlabeled ligands for 2 hr at 22˚C. (Kinetics of [^{3}H]NBI 35965 binding were from Table 1 and the dose set at 1.5 nM. The unlabeled ligand k_{-1} was varied and the k_1 value set at 10 $10^6 M^{-1}min^{-1}$.) Under these conditions, as the residence time of the unlabeled ligand approached and then exceeded the 2 hr incubation time, the apparent affinity approached a limit of about 0.5 nM such that compounds with markedly different k_{-1} and K_i values could no longer be distinguished on the basis of their apparent affinity. This affinity limit matched the apparent boundary of affinity measured experimentally (Fig. 4). We conclude that lack of equilibration underlies the compressed affinity range determined from traditional binding assay conditions.

In vivo pharmacodynamics of CRF_1 receptor antagonists with varying kinetic binding activity – As described above, measuring binding kinetics revealed previously unappreciated differences of receptor binding pharmacology and, for some ligands, exceptionally slow dissociation of the receptor-ligand complex (Table 2, Fig. 4). We next investigated the extent to which this newly revealed *in vitro* binding activity translated to the *in vivo* pharmacology of the ligands. Quantitative pharmacodynamics of CRF_1 receptor antagonism was assessed by measuring plasma ACTH levels in adrenalectomized rats (Fig. 5). This model was used because it allows detection of sustained *in vivo* efficacy (Rivier et al., 1999) using a quantitative biomarker (ACTH).

Sustained, elevated ACTH was observed in adrenalectomized rats out to six hr after vehicle administration (Fig. 5A). The tonic ACTH level was greater than 1000

JPET Fast Forward. Published on February 22, 2012 as DOI: 10.1124/jpet.111.188714
This article has not been copyedited and formatted. The final version may differ from this version.

pg/ml (see legend to Fig. 5), compared with an average of 160 pg/ml in intact animals in our laboratory. This response was blocked by 100 µg astressin, a nonselective peptide CRF_1 / CRF_2 receptor antagonist, but not by 100 µg asressin$_{2B}$, a CRF_2-selective peptide antagonist (data not shown), consistent with activation of the CRF_1 receptor underlying the elevated ACTH level and in agreement with previous studies (Rivier et al., 1999). The effects of nonpeptide antagonists were then evaluated on this prolonged CRF_1 receptor-mediated response. We compared the PK/PD relationship of three ligands, NBI 30775, NBI 34041 and NBI 35965. The apparent affinity of the three ligands was similar when measured with original assay conditions (apparent K_i of 2.6 nM, 1.4 nM and 1.1 nM for NBI 30775, NBI 34041 and NBI 35965, respectively, Table 3, Fig. 4A). The ligands were well differentiated by their dissociation rate constant and kinetically-derived affinity (residence times of 2.2 hr, 53 min and 16 min for NBI 30775, NBI 34041 and NBI 35965, respectively, with corresponding K_i values of 0.36 nM, 2.3 nM and 1.7 nM, Table 2, Fig. 4).

At the highest dose (10 mg/kg), all three ligands reduced ACTH acutely (1 hr post-injection, Fig. 5A-C). After a longer duration a clear difference emerged between NBI 35965 and the other two ligands. The ACTH level returned to the vehicle level by 2 hr for NBI 35965 (Fig. 5C), whereas the response was sustained for 4-6 hr for NBI 30775 and NBI 34041 (Fig. 5A and B). Comparing the time course of compound clearance indicated that the difference between NBI 30775 and NBI 35965 could not be accounted for by pharmacokinetics; the pharmacokinetic profile of the compounds was very similar (Fig. 5D). The more sustained ACTH suppression produced by NBI 30775 compared with NBI 35965 can be explained by prolonged occupancy of the CRF_1 receptor (k_{-1} $t_{1/2}$

JPET Fast Forward. Published on February 22, 2012 as DOI: 10.1124/jpet.111.188714
This article has not been copyedited and formatted. The final version may differ from this version.

of 2.2 hr and compared with 16 min, Table 2, Fig. 4B). At the lower dose of 1 mg/kg, NBI 30775 and NBI 34041 sustainably reduced ACTH by a slightly smaller increment, whereas NBI 35965 had no appreciable effect (Fig. 5A-C). The PK/PD relationship was investigated in more detail by comparing the concentration-effect data of the ligands. The level of ACTH reduction at the time of peak effect (1 hour) was plotted against the plasma concentration of ligand at this time point (Fig. 5E). The rank order of potency was NBI 30775 > NBI 34041 = NBI 35965 (Fig. 5E), the same as that for binding affinity (0.36 nM for NBI 30775, 1.7 nM for NBI 34041 and 2.3 nM for NBI 35965, Table 2). Collectively, the comparative *in vivo* pharmacodynamics can be explained by the kinetics of antagonist binding to the CRF_1 receptor; long sustained duration of action of NBI 30775, compared with NBI 35965, can be explained by the longer receptor residence time; and the higher *in vivo* potency of NBI 30775 is consistent with the higher receptor binding affinity of the ligand.

Kinetic structure-activity relationships of CRF_1 receptor antagonists – We next used kinetic measurements to investigate the structure-activity relationships that ultimately resulted in the development of lead compounds from initial, lower-affinity chemical starting points (Arvanitis et al., 1999; Hodge et al., 1999). SAR studies have identified a number of key structural features of the ligands that result in high affinity interaction with the CRF_1 receptor (reviewed in Gilligan et al., 2000b; Kehne and De Lombaert, 2002), (diagrammatic representation in Fig.9, adapted from the models developed in these studies). We assessed the contribution of the association and dissociation rate constants to the affinity-enhancing role of these elements of chemical structure. (A graphical

JPET Fast Forward. Published on February 22, 2012 as DOI: 10.1124/jpet.111.188714
This article has not been copyedited and formatted. The final version may differ from this version.

representation of these three binding constants is used in Figs. 6-8 to provide a visual tool for evaluating ligand SAR. See legend to Fig. 5 for details.) These features are evident from the common structural groups of the compounds in Fig. 1. A heterocyclic core bears a potential hydrogen-bond acceptor nitrogen atom. Attached to the core is a benzyl group or aromatic heterocycle (the 'lower' or 'pendant' aromatic group), separated from the core nitrogen by a one- or two-atom spacer. The aromatic group is oriented orthogonal to the plain of the core in the bioactive conformation (Hodge et al., 1999). On the opposite side of the core, N-, C- or O-linked groups, often aliphatic, modify receptor binding affinity.

The optimal, orthogonal relationship between the lower aromatic group and the core is maintained by flanking substituents on these rings that enforce this twisted bioactive conformation (Hodge et al., 1999; Gilligan et al., 2000b; Kehne and De Lombaert, 2002). Within the tricyclic series we examined, these substituents are the ortho-position substituent on the lower ring (R1, Fig. 6) and the 4-position substituent on the core pyridine [R2, Fig. 7 (Gross et al., 2005)]. We first investigated the effect of the R1 substituent on the kinetics of binding, using (10S)-9-(cyclopropylmethyl)-10-ethyl-3-(4-fluorophenyl)-6-methyl-1,2,5,9-tetraazatricyclo[6.3.1.$0^{4,12}$]dodeca-2,4,6,8(12)-tetraene (NBI 37608, R1 = H) and (10S)-3-(2-chloro-4-fluorophenyl)-9-(cyclopropylmethyl)-10-ethyl-6-methyl-1,2,5,9-tetraazatricyclo[6.3.1.$0^{4,12}$]dodeca-2,4,6,8(12)-tetraene (NBI 37606, R1 = Cl) (Fig. 6). In the absence of a 2-position substituent, the association rate constant was very low (k_1 of 0.048 $10^6 M^{-1}min^{-1}$ for NBI 37608, Fig. 6), indicating a substantial kinetic barrier to ligand association. Substitution at the ortho position with Cl reduced this barrier, increasing the association rate by 33-

JPET Fast Forward. Published on February 22, 2012 as DOI: 10.1124/jpet.111.188714
This article has not been copyedited and formatted. The final version may differ from this version.

fold (to 1.6 $10^6 M^{-1}min^{-1}$, NBI 37606, Fig. 6). These kinetic data support the model developed previously in Fig. 9, that the binding pocket in the receptor for the lower aromatic ring is constrained relative to the binding site for the core. The pocket is too rigid to accommodate the freely-rotating lower aromatic of NBI 37608, so successful collision is limited by the low probability that the group is rotated to the optimal orthogonal position by chance when the ligand encounters the receptor (Fig. 9), manifested as a low k_1 value (Fig. 6). Constraining the lower aromatic in the orthogonal position (NBI 37606) optimizes the presentation of this group to the postulated rigid binding pocket on the receptor (Fig. 9), resulting in a greater frequency of successful collisions with the receptor, manifested as an increase of k_1. The ortho-substituent did not significantly affect ligand dissociation (Fig. 6), suggesting it does not contribute to stabilizing the receptor-ligand complex once the ligand has associated with the receptor. In combination, the rate constants indicate the affinity-enhancing effect of the ortho-substituent was driven by an increase of k_1.

We next examined the R2 substituent flanking the core pyridine (Fig. 7). This small substituent on the ligand core increases CRF_1 receptor affinity in a variety of ligand structures (Arvanitis et al., 1999; Gilligan et al., 2000b; Kehne and De Lombaert, 2002). We investigated the kinetics of the affinity enhancement using non-substituted 3-(2,4-dichlorophenyl)-9-(heptan-4-yl)-1,2,5,9-tetraazatricyclo[6.3.1.$0^{4,12}$]dodeca-2,4,6,8(12)-tetraene (NBI 49721, R2 = H) and NBI 34041 (R2 = CH_3) (Fig. 7). The k_1 value of NBI 49721 was exceptionally low (0.12 $10^6 M^{-1}min^{-1}$, Fig. 7) implying a poorly-configured structure for successful collision with the receptor. Substitution of H of NBI 49721 with the methyl group of NBI 34041 increased k_1 69-fold, a similar magnitude to the effect of

JPET Fast Forward. Published on February 22, 2012 as DOI: 10.1124/jpet.111.188714
This article has not been copyedited and formatted. The final version may differ from this version.

ortho-substitution of the lower aromatic (33-fold, Fig. 6). This increased association is consistent with the core methyl substituent stabilizing the orthogonal relationship of the lower aromatic group with respect to the core, increasing the probability of successful collision of this group with a rigid binding pocket on the receptor (Fig. 9). The core methyl substituent also significantly slowed dissociation (decreased k_{-1}, Fig. 7), implying the methyl substituent stabilizes the receptor-ligand complex. This finding is consistent with the methyl group interacting with a hydrophobic pocket on the receptor (Fig. 9), likely small given the size constraint at this position in the ligand pharmacophore (Arvanitis et al., 1999; Hodge et al., 1999; Gilligan et al., 2000b; Kehne and De Lombaert, 2002). In combination, the rate constants indicate the affinity-enhancing effect of the core-flanking R2 substituent resulted from increasing k_1 and decreasing k_{-1}.

In early SAR studies ligand affinity was increased by the presence of branched alkyl or heteroalkyl chains on the opposite side of the core from the lower aromatic group. The effect on affinity of these 'upper' aliphatic groups was dependent on their size, branching pattern and, where a chiral center was present, the stereochemical configuration (Gilligan et al., 2000a; Gross et al., 2005). We evaluated the kinetics underlying the affinity contribution of the upper aliphatic groups at the R3 position of the NBI 34041 scaffold (Fig. 8). A small, 3-carbon aliphatic group in this position (3-(2,4-dichlorophenyl)-6-methyl-9-(propan-2-yl)-1,2,5,9-tetraazatricyclo[6.3.1.$0^{4,12}$]dodeca-2,4,6,8(12)-tetraene, NBI 78194 of Fig. 8) bound weakly to the receptor (K_i of 200 nM) owing to a low value of k_1 (0.12 $10^6 M^{-1}min^{-1}$) and rapid dissociation (k_{-1} $t_{1/2}$ of 1 min). Increasing the chain length to 5 methylene units (3-(2,4-dichlorophenyl)-6-methyl-9-(pentan-3-yl)-1,2,5,9-tetraazatricyclo[6.3.1.$0^{4,12}$]dodeca-2,4(12),5,7-tetraene, NBI 34417

of Fig. 8) increased affinity 16-fold. Underlying this increase was an 18-fold increase of k_1 and a 4-fold slowing of dissociation (Fig. 8). The former implies the addition of the methylene units reduces a kinetic barrier in the association pathway. The latter implies the longer alkyl chain increases the stability of the receptor-ligand complex, possibly by anchoring this region of the ligand within a hydrophobic binding pocket (Gross et al., 2005) (Fig. 9). Extension to 7 methylene units (NBI 34041) slowed dissociation 3.0-fold, suggesting a slightly stronger stabilizing interaction, without appreciably affecting association (Fig. 8). Extending the chain to 9 methylene units (3-(2,4-dichlorophenyl)-6-methyl-9-(nonan-5-yl)-1,2,5,9-tetraazatricyclo[6.3.1.$0^{4,12}$]dodeca-2,4(12),5,7-tetraene, NBI 34416 of Fig 8) reduced affinity by decreasing k_1 18-fold and by accelerating dissociation 3.8-fold (Fig. 8), indicating a size constraint on the binding kinetics. Constraining the aliphatic group in a cyclohexyl ring (9-cyclohexyl-3-(2,4-dichlorophenyl)-6-methyl-1,2,5,9-tetraazatricyclo[6.3.1.$0^{4,12}$]dodeca-2,4(12),5,7-tetraene, NBI 34802 of Fig. 8) decreased k_1 and increased k_{-1} suggesting flexibility of the aliphatic region is necessary for optimal association with and dissociation from the receptor. Interestingly, the binding kinetics of the 3-propyl, 5-nonyl and cyclohexyl analogues were similar (Fig. 8), suggesting optimal size and flexibility are required for successful collision of the upper aliphatic group with the receptor.

Overall the kinetic SAR indicates that the improvement of affinity in the tricyclic series has resulted from an increase of k_1 together with a decrease of k_{-1}. In all three regions of the receptor we investigated, optimizing the groups increased k_1. The association rate constant of even the most optimized compounds was low (highest k_1 of 20 $10^6 M^{-1}min^{-1}$, for NBI 35965, Table 2) relative to the diffusion-limited rate constant

[approximately 10,000 $10^6 M^{-1} min^{-1}$ (Copeland et al., 2006)]. The kinetic data reveal that the development of high affinity ligands has involved increasing k_1 about 100-fold. Given the exceptionally low k_1 values of the starting points (100,000-fold less than diffusion), the remaining shortfall of k_1 in high-affinity compounds is made up for by the unusually long residence times (up to 53 min, for NBI 34041, Table 2).

JPET Fast Forward. Published on February 22, 2012 as DOI: 10.1124/jpet.111.188714
This article has not been copyedited and formatted. The final version may differ from this version.

Discussion

The CRF system is the principal regulator of stress responses (Bale and Vale, 2004). Drug discovery has yielded CRF_1 receptor antagonists as potential treatments for depression and other disorders of the stress axis (Holsboer, 2000; Grigoriadis, 2005). Testing the utility of this mechanism will be aided by designing antagonists with maximal efficacy for blocking the actions of CRF at the CRF_1 receptor. Prolonging receptor residence time is one approach for achieving strong *in vivo* and clinical efficacy (Copeland et al., 2006; Vauquelin and Van Liefde, 2006; Brinkerhoff et al., 2008). This approach requires an understanding of the kinetics of receptor-ligand interaction. In this study we re-evaluated the pharmacology of previously-identified CRF_1 antagonists in the context of their receptor binding kinetics.

Measuring binding kinetics of twelve lead compounds redefined their binding pharmacology (summarized in Fig. 4). No appreciable differences of affinity between the compounds have been noted previously but the kinetic affinity (k_{-1} / k_1) ranged 510-fold, from 49 pM for SSR125543A to 25 nM for NBI 27914 (Table 1). Long ligand residence times likely compressed the observed affinity range in previously-utilized assays, which employed relatively short incubations at room temperature. The wide range of affinity resulted in large part from the range of residence time, from 7.2 hours for SSR125543A to 2.6 min for NBI 27914 (Fig. 4, Table 1). Three compounds bound with an unusually slow residence time of greater than 1 hr at 37°C (SSR125543A, NBI 30775 and DMP-904). While slow ligand dissociation at room temperature has been reported for numerous GPCRs (Anthes et al., 2002; Fierens et al., 2002; Dowling and Charlton, 2006; Tummino and Copeland, 2008), including the CRF_1 receptor (Miller et al., 2011; Ramsey et al.,

JPET Fast Forward. Published on February 22, 2012 as DOI: 10.1124/jpet.111.188714
This article has not been copyedited and formatted. The final version may differ from this version.

2011), few studies reported k_{-1} at the physiologic temperature. In the most studied case for GPCRs, at 37°C candesartan dissociates from the AT_1 receptor with a k_{-1} $t_{1/2}$ of 58 min (Fierens et al., 2002).

The redefinition of lead compound binding activity modifies the interpretation of *in vivo* efficacy. For example, in a recent study (Ramsey et al., 2011), the *in vivo* EC_{50} for occupancy of the CRF_1 receptor was correlated with the kinetically-defined affinity. In the present study, newly-revealed differences of binding activity explained differential compound pharmacodynamics for suppressing ACTH in adrenalectomized rats. The rank order of efficacy (NBI 30775 > NBI 34041 = NBI 35965, Fig. 5E) was the same as the rank order of kinetically-defined binding affinity (Fig. 4A, Table 2). Prolonged suppression of ACTH was observed with NBI 30775 but not NBI 35965 (Fig5. A and C), despite their nearly identical pharmacokinetic profiles (Fig. 5D), consistent with the sustained antagonism of NBI 30775 resulting from its long residence time (Fig. 4B, Table 2) (Vauquelin and Van Liefde, 2006). It is worth noting that ACTH provides a biomarker that can be translated from preclinical to clinical pharmacology.

Conceivably, the kinetic redefinition CRF_1 receptor-antagonist interaction might impact interpretation of ligand efficacy in humans. Comparison of clinical efficacy between compounds will need to consider differences of accurately-determined binding affinity. The kinetically-derived affinity measurement unmasked differences between compounds tested clinically to date; NBI 30775 binds with 33-fold higher affinity than CP-316,311 and 53-fold higher affinity than pexacerfont (Fig. 4A, Table 2). With respect to the dissociation rate constant, in the study of Ramsey et al. k_{-1} was used in a PK/PD simulation to suggest appreciable occupancy (>50%) was not achieved in the human

JPET Fast Forward. Published on February 22, 2012 as DOI: 10.1124/jpet.111.188714
This article has not been copyedited and formatted. The final version may differ from this version.

behavioral and endocrine trial of NBI 30775 (Zobel et al., 2000; Kunzel et al., 2003; Ramsey et al., 2011). [NBI 30775 did not significantly affect plasma ACTH in these patients (Kunzel et al., 2003).] Comparison with other receptor systems suggests the residence time could impact human pharmacodynamics. At the AT_1 receptor, the slowly-dissociating antagonist candesartan produces a greater maximal antihypertensive effect than the more rapidly dissociating antagonist losartan (Hansson, 2001), and elicits a prolonged effect that endures sufficiently to tolerate a missed dose in humans (Lacourciere and Asmar, 1999). The prolonged pharmacodynamics of the μ-opioid receptor partial agonist buprenorphine, used for managing opiate withdrawal, might result in part from slow dissociation from the receptor (Yassen et al., 2006). A long residence time has been posited to explain the prolonged efficacy of the M3 antagonist tiotropium (Dowling and Charlton, 2006), used to treat chronic obstructive pulmonary disease. The long-acting antihistamine desloratadine (the active metabolite of loratadine) dissociates slowly from the H_1 receptor (Anthes et al., 2002). It is tempting to speculate that a long residence time of a CRF_1 receptor antagonist might aid the detection of a measurable and/or prolonged effect in humans, on endocrine biomarkers (e.g. ACTH) or on scores of psychiatric dysfunction.

Application of binding kinetic information will aid medicinal chemistry strategies for the future optimization of CRF_1 receptor antagonists. For most receptor-ligand interactions, the association rate is diffusion-limited and ligand SAR is driven by changes in the dissociation rate (Tummino and Copeland, 2008). By contrast, for CRF_1 receptor antagonists the association rate is limited by ligand interaction with the receptor. This conclusion is based on the k_1 value being at least 300-fold lower than rate of diffusion; k_1

JPET Fast Forward. Published on February 22, 2012 as DOI: 10.1124/jpet.111.188714
This article has not been copyedited and formatted. The final version may differ from this version.

being highly dependent on the chemical structure of the ligand (Table 2, Figs. 6-8); and k_1 SAR being consistent with previously-described models of small molecule interaction with the CRF_1 receptor (Fig. 9, Gilligan et al., 2000b; Kehne and De Lombaert, 2002). [More refined models, such as those being developed for the H_1 receptor (Wittmann et al., 2011), will require structural information on the CRF_1 receptor or a homologous Class B GPCR.] Collectively, the retrospective kinetic SAR indicates affinity-improving changes overcame kinetic barriers in the ligand association pathway (for example, restricting rotational freedom of the lower aromatic ring) and stabilized the receptor-ligand interaction (optimizing 'upper' aliphatic chain length).

Unusual binding kinetic behavior can be a manifestation of a more complex binding mechanism than a simple one-step binding and dissociation process (mechanism A in Tummino and Copeland, 2008). In a two-step binding model, (mechanism B), ligand associates with and dissociates from the receptor in an initial complex (defined by the rate constants k_1 and k_2) which then undergoes a transition to form a final complex (formation defined by k_3, deformation by k_4). A common manifestation of this model in kinetic data is a hyperbolic dependence of the observed association rate on the ligand concentration (Strickland et al., 1975; Tummino and Copeland, 2008). Here the dependence was linear up to a radioligand concentration of 20 nM for [^{3}H]NBI 30775 and 45 nM for [^{3}H]NBI 359655, albeit at room temperature. According to simulations we have performed, the two-step model can apply to these data when the initial interaction is transient (large values of k_1 and k_2) and when k_3 is > 30-fold k_4. Under these conditions, the final complex predominates, the observed dissociation rate constant is almost equal to k_4, and k_1, k_2 and k_3 define the observed association rate constant. Using these inferences,

JPET Fast Forward. Published on February 22, 2012 as DOI: 10.1124/jpet.111.188714
This article has not been copyedited and formatted. The final version may differ from this version.

the two-step model can provide a simple mechanistic explanation for the kinetic SAR; ligand associates rapidly with the receptor (diffusion limited) to form an initial state, from which it also dissociates rapidly. This state then transitions into the final complex, with the structure of the ligand defining k_3 and k_4, and hence the observed association and dissociation rate constants. In a third model, mechanism C (Tummino and Copeland, 2008), the receptor transitions between two states, one that binds ligand, one that does not. For the CRF_1 receptor as for all Class B GPCRs, the large N-terminal domain could act as a gate that needs to open to allow access of small molecules to the membrane-spanning domain of the receptor, a process consistent with Mechanism C. Deletion of the N-terminal domain (Hoare et al., 2004) did not appreciably affect k_1 and k_{-1} of [^{3}H]NBI 30775 (data not shown), suggesting this domain is not responsible for the unusual kinetics of small molecule binding to the CRF_1 receptor.

In summary, investigating CRF_1 receptor binding kinetics redefined the pharmacology of CRF_1 receptor antagonists. By overcoming artificial compression of affinity measurement due to lack of equilibration, substantial differences of the binding behavior between lead compounds was revealed. These differences translated to differential pharmacodynamics *in vivo*. Very slow ligand dissociation was observed that could maximize compound efficacy and prolong the duration of efficacy. The molecular basis of ligand SAR in the evolution of these compounds involved spatial constraint of the ligand and potentially the binding pocket in the receptor, and kinetic barriers in the association pathway that were lowered by optimizing ligand structure. Applying this new knowledge of CRF_1 receptor-ligand interactions will aid future development of therapeutic ligands targeting this receptor.

JPET Fast Forward. Published on February 22, 2012 as DOI: 10.1124/jpet.111.188714

JPET Fast Forward. Published on February 22, 2012 as DOI: 10.1124/jpet.111.188714
This article has not been copyedited and formatted. The final version may differ from this version.

Acknowledgements

The authors gratefully acknowledge Jacek Slon-Usakiewicz for FAC-MS data and John P Williams for valuable guidance and discussion.

Authorship Contributions

Participated in research design: Fleck, Hoare, Bradbury, Grigoriadis

Conducted experiments: Fleck, Hoare, Pick

Contributed new reagents or analytic tools: Fleck, Pick

Performed data analysis: Fleck, Hoare, Pick

Wrote or contributed to the writing of the manuscript: Hoare, Fleck, Grigoriadis

References

Anthes JC, Gilchrest H, Richard C, Eckel S, Hesk D, West RE, Jr., Williams SM, Greenfeder S, Billah M, Kreutner W and Egan RE (2002) Biochemical characterization of desloratadine, a potent antagonist of the human histamine H(1) receptor. *Eur J Pharmacol* **449**:229-237.

Aranyi P and Quiroga V (1980) Determine rate constants of interaction of steroid receptors with non-labelled ligands. *J Steroid Biochem* **13**:1167-1172.

Arvanitis AG, Gilligan PJ, Chorvat RJ, Cheeseman RS, Christos TE, Bakthavatchalam R, Beck JP, Cocuzza AJ, Hobbs FW, Wilde RG, Arnold C, Chidester D, Curry M, He L, Hollis A, Klaczkiewicz J, Krenitsky PJ, Rescinito JP, Scholfield E, Culp S, De Souza EB, Fitzgerald L, Grigoriadis D, Tam SW, Wong YN, Huang SM and Shen HL (1999) Non-peptide corticotropin-releasing hormone antagonists: syntheses and structure-activity relationships of 2-anilinopyrimidines and -triazines. *J Med Chem* **42**:805-818.

Bale TL and Vale WW (2004) CRF And CRF Receptors: Role in Stress Responsivity and Other Behaviors. *Annu Rev Pharmacol Toxicol* **44**:525-557.

Binneman B, Feltner D, Kolluri S, Shi Y, Qiu R and Stiger T (2008) A 6-week randomized, placebo-controlled trial of CP-316,311 (a selective CRH1 antagonist) in the treatment of major depression. *Am J Psychiatry* **165**:617-620.

Brinkerhoff CJ, Choi JS and Linderman JJ (2008) Diffusion-limited reactions in G-protein activation: unexpected consequences of antagonist and agonist competition. *J Theor Biol* **251**:561-569.

Christopoulos A (1998) Assessing the distribution of parameters in models of ligand-receptor interaction: to log or not to log. *Trends Pharmacol Sci* **19**:351-357.

Copeland RA, Pompliano DL and Meek TD (2006) Drug-target residence time and its implications for lead optimization. *Nat Rev Drug Discov* **5**:730-739.

Coric V, Feldman HH, Oren DA, Shekhar A, Pultz J, Dockens RC, Wu X, Gentile KA, Huang SP, Emison E, Delmonte T, D'Souza BB, Zimbroff DL, Grebb JA, Goddard AW and Stock EG (2010) Multicenter, randomized, double-blind, active comparator and placebo-controlled trial of a corticotropin-releasing factor receptor-1 antagonist in generalized anxiety disorder. *Depress Anxiety* **27**:417-425.

Dowling MR and Charlton SJ (2006) Quantifying the association and dissociation rates of unlabelled antagonists at the muscarinic M3 receptor. *Br J Pharmacol* **148**:927-937.

Fierens FL, Vanderheyden PM, Roggeman C, Vande Gucht P, De Backer JP and Vauquelin G (2002) Distinct binding properties of the AT(1) receptor antagonist [(3)H]candesartan to intact cells and membrane preparations. *Biochem Pharmacol* **63**:1273-1279.

Gilligan PJ, Baldauf C, Cocuzza A, Chidester D, Zaczek R, Fitzgerald LW, McElroy J, Smith MA, Shen HS, Saye JA, Christ D, Trainor G, Robertson DW and Hartig P (2000a) The discovery of 4-(3-pentylamino)-2,7-dimethyl-8-(2-methyl-4-methoxyphenyl)-pyrazolo-[1 ,5-a]-pyrimidine: a corticotropin-releasing factor (hCRF1) antagonist. *Bioorg Med Chem* **8**:181-189.

Gilligan PJ, Robertson DW and Zaczek R (2000b) Corticotropin releasing factor (CRF) receptor modulators: progress and opportunities for new therapeutic agents. *J Med Chem* **43**:1641-1660.

Grigoriadis DE (2005) The corticotropin-releasing factor receptor: a novel target for the treatment of depression and anxiety-related disorders. *Expert Opin Ther Targets* **9**:651-684.

Gross RS, Guo Z, Dyck B, Coon T, Huang CQ, Lowe RF, Marinkovic D, Moorjani M, Nelson J, Zamani-Kord S, Grigoriadis DE, Hoare SR, Crowe PD, Bu JH, Haddach M, McCarthy J, Saunders J, Sullivan R, Chen T and Williams JP (2005) Design and synthesis of tricyclic corticotropin-releasing factor-1 antagonists. *J Med Chem* **48**:5780-5793.

Hansson L (2001) The relationship between dose and antihypertensive effect for different AT1-receptor blockers. *Blood Press Suppl*:33-39.

Hoare SR, Sullivan SK, Ling N, Crowe PD and Grigoriadis DE (2003) Mechanism of corticotropin-releasing factor type I receptor regulation by nonpeptide antagonists. *Mol Pharmacol* **63**:751-765.

Hoare SR, Sullivan SK, Schwarz DA, Ling N, Vale WW, Crowe PD and Grigoriadis DE (2004) Ligand affinity for amino-terminal and juxtamembrane domains of the corticotropin releasing factor type I receptor: regulation by G-protein and nonpeptide antagonists. *Biochemistry* **43**:3996-4011.

Hodge CN, Aldrich PE, Wasserman ZR, Fernandez CH, Nemeth GA, Arvanitis A, Cheeseman RS, Chorvat RJ, Ciganek E, Christos TE, Gilligan PJ, Krenitsky P, Scholfield E and Strucely P (1999) Corticotropin-releasing hormone receptor

antagonists: framework design and synthesis guided by ligand conformational studies. *J Med Chem* **42**:819-832.

Holsboer F (2000) The corticosteroid receptor hypothesis of depression. *Neuropsychopharmacology* **23**:477-501.

Kehne J and De Lombaert S (2002) Non-peptidic CRF1 receptor antagonists for the treatment of anxiety, depression and stress disorders. *Curr Drug Target CNS Neurol Disord* **1**:467-493.

Kenakin T (2007) Collateral efficacy in new drug discovery. *Trends Pharmacol Sci* **28**:359-361.

Kunzel HE, Zobel AW, Nickel T, Ackl N, Uhr M, Sonntag A, Ising M and Holsboer F (2003) Treatment of depression with the CRH-1-receptor antagonist R121919: endocrine changes and side effects. *J Psychiatr Res* **37**:525-533.

Lacourciere Y and Asmar R (1999) A comparison of the efficacy and duration of action of candesartan cilexetil and losartan as assessed by clinic and ambulatory blood pressure after a missed dose, in truly hypertensive patients: a placebo-controlled, forced titration study. Candesartan/Losartan study investigators. *Am J Hypertens* **12**:1181-1187.

Li YW, Fitzgerald L, Wong H, Lelas S, Zhang G, Lindner MD, Wallace T, McElroy J, Lodge NJ, Gilligan P and Zaczek R (2005) The pharmacology of DMP696 and DMP904, non-peptidergic CRF1 receptor antagonists. *CNS Drug Rev* **11**:21-52.

Miller DC, Klute W and Brown AD (2011) Discovery of potent, metabolically stable purine CRF-1 antagonists with differentiated binding kinetic profiles. *Bioorg Med Chem Lett* **21**:6108-6111.

Motulsky HJ and Mahan LC (1984) The kinetics of competitive radioligand binding predicted by the law of mass action. *Mol Pharmacol* **25**:1-9.

Paton WDM (1966) A kinetic approach to the mechanism of drug action. *Adv Drug Res* **3**:57-80.

Ramsey SJ, Attkins NJ, Fish R and van der Graaf PH (2011) Quantitative pharmacological analysis of antagonist binding kinetics at CRF(1) receptors in vitro and in vivo. *Br J Pharmacol* **164**:992-1007.

Rivier JE, Kirby DA, Lahrichi SL, Corrigan A, Vale WW and Rivier CL (1999) Constrained corticotropin releasing factor antagonists (astressin analogues) with long duration of action in the rat. *J Med Chem* **42**:3175-3182.

Rocha e S (1969) A thermodynamic approach to problems of drug antagonism I. The "Charniere theory". *Eur J Pharmacol* **6**:294-302.

Slon-Usakiewicz JJ, Ng W, Dai JR, Pasternak A and Redden PR (2005) Frontal affinity chromatography with MS detection (FAC-MS) in drug discovery. *Drug Discov Today* **10**:409-416.

Strickland S, Palmer G and Massey V (1975) Determination of dissociation constants and specific rate constants of enzyme-substrate (or protein-ligand) interactions from rapid reaction kinetic data. *J Biol Chem* **250**:4048-4052.

Sykes DA, Dowling MR and Charlton SJ (2009) Exploring the mechanism of agonist efficacy: a relationship between efficacy and agonist dissociation rate at the muscarinic M3 receptor. *Mol Pharmacol* **76**:543-551.

Tummino PJ and Copeland RA (2008) Residence time of receptor-ligand complexes and its effect on biological function. *Biochemistry* **47**:5481-5492.

Vauquelin G and Van Liefde I (2006) Slow antagonist dissociation and long-lasting in vivo receptor protection. *Trends Pharmacol Sci* **27**:356-359.

Verheijen I, Vanderheyden PM, De Backer JP and Vauquelin G (2004) AT1 receptor antagonists. *Curr Med Chem Cardiovasc Hematol Agents* **2**:69-77.

Wittmann HJ, Seifert R and Strasser A (2011) Influence of the N-terminus and the E2-loop onto the binding kinetics of the antagonist mepyramine and the partial agonist phenoprodifen to H(1)R. *Biochem Pharmacol* **82**:1910-1918.

Yassen A, Olofsen E, Romberg R, Sarton E, Danhof M and Dahan A (2006) Mechanism-based pharmacokinetic-pharmacodynamic modeling of the antinociceptive effect of buprenorphine in healthy volunteers. *Anesthesiology* **104**:1232-1242.

Zobel AW, Nickel T, Kunzel HE, Ackl N, Sonntag A, Ising M and Holsboer F (2000) Effects of the high-affinity corticotropin-releasing hormone receptor 1 antagonist R121919 in major depression: the first 20 patients treated. *J Psychiatr Res* **34**:171-181.

Zorrilla EP and Koob GF (2010) Progress in corticotropin-releasing factor-1 antagonist development. *Drug Discov Today* **15**:371-383.

Footnotes

* BAF and SRJH contributed equally on this manuscript.

JPET Fast Forward. Published on February 22, 2012 as DOI: 10.1124/jpet.111.188714
This article has not been copyedited and formatted. The final version may differ from this version.

Legends for Figures

Fig. 1. **Chemical structure of lead CRF_1 receptor nonpeptide antagonists.** Compounds with their name underlined have been tested in clinical trials CP-316,311 (Binneman et al., 2008); NBI 30775 (Zobel et al., 2000); and pexacerfont - (Coric et al., 2010). See Materials and Methods for chemical name of compounds.

Fig. 2. **Radiolabeled nonpeptide antagonist dissociation from and association with the CRF_1 receptor.** Specific radioligand binding to the CRF_1 receptor was measured at 22°C and 37°C as described in Materials and Methods, over the time course of radioligand dissociation (A) and association (B). Data are from representative experiments performed 2-5 times. Data were fit to mono-exponential and bi-exponential equations and in all cases the mono-exponential fits (to eqs. 1 and 2), shown in the figure, provided the best fit to the data ($p > 0.05$, partial F-test). For the association experiments in B, approximately equivalent concentrations of radioligand were used (3.8 nM for [^{3}H]NBI 30775 at 22°C, 2.9 nM for [^{3}H]NBI 35965 at 22°C, 3.1 nM for [^{3}H]NBI 30775 at 37°C and 5.5 nM for [^{3}H]NBI 35965 at 37 °C). See Materials and Methods for chemical name of compounds.

Fig. 3. **Measurement of binding kinetics of unlabeled nonpeptide ligands at the CRF_1 receptor at 37°C.** The data illustrate the binding data for lead compounds with a range of residence times (see Table 2): A, NBI 27914 (k_{-1} $t_{1/2}$ value of 2.6 min); B, NBI 35965 (16 min); C, NBI 30775 (2.2 hr) and SSR125543A (7.2 hr). The time course of

association of specific CRF_1 receptor binding was measured as described in Materials and Methods, in the absence of nonpeptide ligand and in the presence of a range of four or five concentrations of unlabeled ligand at 37°C. The same experimental conditions were used for the experiment in Fig. 2, [^{3}H]NBI 30775 data at 37°C. Data were analyzed globally using eq. 5 to determine the association rate constant and dissociation rate constant of the unlabeled ligands. In the experiments shown, the global r^2 value of the fit was 0.93 for NBI 27914 (A), 0.94 for NBI 35965 (B), 0.94 for NBI 30775 (C) and 0.94 for SSR125543A (D). Data are from representative experiments performed 3-16 times. See Materials and Methods for chemical name of compounds.

Fig. 4. **Binding kinetic characterization of lead CRF_1 receptor antagonists.** Lead compounds were selected based on progression to advanced preclinical or early clinical testing (Fig. 1). Data are from Tables 2 and 3. A. Comparison of affinity measurements for lead compounds. 'Traditional assay (disequilibrium)' refers to apparent affinity determined using traditional binding assay conditions (competition versus ^{125}I-sauvagine at 22 °C for 2 hr, Table 3). 'True K_i (kinetic)' refers to the kinetic K_i (k_{-1} / k_1) at 37°C, measured using competitions kinetics vs [^{3}H]NBI 30775 as described in Fig. 3 and Table 2. B. Comparison of residence time. Clinically-tested compounds are highlighted (solid lines for NBI 30775, and dashed lines for CP-316,311 and pexacerfont). Residence time (k_{-1} $t_{½}$) was measured using competitions kinetics vs [^{3}H]NBI 30775 as described Fig. 3 and Table 2. See Materials and Methods for chemical name of compounds.

Fig. 5. ***In vivo*** **pharmacology of CRF_1 receptor antagonists: Inhibition of plasma ACTH in adrenalectomized rats.** Compound or vehicle was administered intravenously. Prior to injection, blood was drawn from every animal and ACTH measured providing the measure 'ACTH at 0 hr.' Data were normalized for each animal by dividing the ACTH level at the specified time point by its ACTH at 0 hr. The mean and standard error, shown in panels A-C, of these intra-animal normalized data were then calculated. A) NBI 30775. ACTH values at 0 hr in pg/ml were 1300 ± 200 for vehicle (n=7), 1600 ± 200 for 1 mg/kg (n=8), and 1700 ± 200 for 10 mg/kg (n=6). B) NBI 34041. ACTH values at 0 hr in pg/ml were 1300 ± 200 for vehicle (n=11), 1200 ± 100 for 1 mg/kg (n=12), and 1600 ± 200 for 10 mg/kg (n=12). C) NBI 35965. ACTH values at 0 hr in pg/ml, were 2000 ± 300 for vehicle (n=8), 1800 ± 100 for 1 mg/kg (n=8), and 1700 ± 300 for 10 mg/kg (n=7). D) Plasma ligand concentrations of NBI 30775, NBI 34041 and NBI 35965. E) Concentration-effect data at time of peak response (1 hr post-injection). See Materials and Methods for chemical name of compounds.

Fig. 6. **Effect of ortho-position substitution of the lower aromatic ring on CRF_1 receptor binding kinetics and affinity of a tricyclic antagonist.** Binding kinetics of the two tricyclic antagonists was measured as described in Materials and Methods. See Materials and Methods for chemical name of compounds. The diagram presents the three binding constants of the ligand. The light grey-filled bar on the left-hand side indicates the dissociation rate constant, the dark grey-filled bar on the right indicates the association rate constant, and the width of the whole bar indicates the affinity. These values are represented as the $\log_{10}$ of their value, presented on the x-axis. The value of the

JPET Fast Forward. Published on February 22, 2012 as DOI: 10.1124/jpet.111.188714
This article has not been copyedited and formatted. The final version may differ from this version.

left-hand edge of the bar is the $\log_{10}$ of the dissociation rate constant (min^{-1}) and the value of the bar's right-hand edge is the $\log_{10}$ of the association rate constant ($M^{-1}.min^{-1}$). The width of the bar is $\log_{10}$ of the affinity constant (pK_i,). Also shown are the numerical data of the values, given as mean ± s.e.m. of the values from multiple experiments (n=3 for both ligands). pK_i was determined from each individual experiment, involving division of k_{-1} by k_1 to determine K_i (eqn. 7), then the average and standard error of the pK_i values were calculated. Statistical comparison of k_{-1} and log k_1 values was performed for all compounds in Figs 6, 7 & 8 combined, using one-way analysis of variance ($p < 0.001$ in both cases). For k_{-1}, the Newman-Keuls multiple comparison post-test indicated the values for NBI 37608 and NBI 37606 were not significantly different ($p > 0.05$) whereas the log k_1 values were ($p < 0.001$). See legend to Fig. 8 for full comparison within the post-test.

Fig. 7. **Effect of flanking core methyl substituent on CRF_1 receptor binding kinetics and affinity of a tricyclic antagonist.** Binding kinetics of the two tricyclic antagonists was measured as described in Materials and Methods. See Materials and Methods for chemical name of compounds. See legend to Fig. 6 for the description of the binding constant diagram. The numerical data are mean ± s.e.m. (n=3 for NBI 49721, n=5 for NBI 34041). pK_i was determined from each individual experiment, involving division of k_{-1} by k_1 to determine K_i (eqn. 7), then the average and standard error of the pK_i values were calculated. Statistical comparison of k_{-1} and log k_1 values was performed for all compounds in Figs 6, 7 & 8 combined, using one-way analysis of variance ($p < 0.001$ in both cases). For k_{-1}, the Newman-Keuls multiple comparison post-test indicated the

JPET Fast Forward. Published on February 22, 2012 as DOI: 10.1124/jpet.111.188714
This article has not been copyedited and formatted. The final version may differ from this version.

values for NBI 49721 and NBI 34041 were significantly different ($p < 0.01$) as were the log k_1 values ($p < 0.001$). See legend to Fig. 8 for full comparison within the post-test.

Fig. 8. **Kinetic SAR of the upper aliphatic group at the R3 position.** Binding kinetics of the tricyclic antagonists was measured as described in Materials and Methods. See Materials and Methods for chemical name of compounds. See legend to Fig. 6 for the description of the binding constant diagram. The numerical data given are mean ± s.e.m. (n=3 for NBI 78194 and NBI 34417, n=2 for NBI 34416 and NBI 34802, and n=5 for NBI 34041). pK_i was determined from each individual experiment, involving division of k_{-1} by k_1 to determine K_i (eqn. 7), then the average and standard error of the pK_i values were calculated. Statistical comparison of k_{-1} and log k_1 values was performed for all compounds in Figs 6, 7 & 8 combined, using one-way analysis of variance ($p < 0.001$ in both cases). For log k_1, the Newman-Keuls multiple comparison post-test indicated the following pairs of values were significantly different: NBI 78194 vs NBI 34417 ($p <0.001$); NBI 78194 vs NBI 34041 ($p < 0.001$). For k_{-1}, the post-test indicated the values for NBI 78194 and NBI 34041 were significantly different ($p < 0.05$). Statistically-significant differences from the Newman-Keuls multiple comparison post-test between compounds in Figs 6 and 7, 6 and 8, or 7 and 8 are as follows: k_{-1}, NBI 37608 vs NBI 34041 ($p < 0.01$), NBI 37608 vs NBI 34417 ($p < 0.05$), NBI 37608 vs NBI 34416 ($p < 0.05$), NBI 49721 vs NBI 34417 ($p < 0.05$), NBI 49721 vs NBI 34416 ($p < 0.05$). log k_1, NBI 37608 vs NBI 49721 ($p < 0.05$), NBI 37608 vs NBI 34041 ($p < 0.001$), NBI 37608 vs NBI 78194 ($p < 0.001$), NBI 37608 vs NBI 34417 ($p < 0.001$), NBI 37608 vs NBI

34416 ($p < 0.001$), NBI 37606 vs NBI 49721 ($p < 0.05$), NBI 37606 vs NBI 34041 ($p < 0.001$), NBI 37606 vs NBI 34417 ($p < 0.001$), NBI 37606 vs NBI 34802 ($p < 0.05$), NBI 49721 vs NBI 78194 ($p < 0.01$), NBI 49721 vs NBI 34417 ($p < 0.001$), NBI 49721 vs NBI 3441 ($p < 0.05$), NBI 49721 vs NBI 34802 ($p < 0.05$).

Fig. 9. **Diagram of putative binding pockets on the CRF_1 receptor for functional groups implicated in kinetic structure-activity relationships of nonpeptide antagonists.** This diagram is adapted from Gilligan et al., 2000b; Kehne and De Lombaert, 2002, based on the comprehensive analysis of ligand SAR in these reviews. The compound shown is NBI 34041.

JPET Fast Forward. Published on February 22, 2012 as DOI: 10.1124/jpet.111.188714
This article has not been copyedited and formatted. The final version may differ from this version.

Tables

Table 1. **Comparison of CRF_1 receptor binding kinetics of labeled and unlabeled antagonists at 22°C and 37°C.**

Ligand	k_{-1}, min^{-1}	Dissociation $t_{1/2}$, min	k_1, $10^6 M^{-1} min^{-1}$	K_d or K_i [a], nM
22°C				
[^{3}H]NBI 35965	0.0023 ± 0.0004	300	4.0 ± 0.8	0.58
NBI 35965 [b]	0.0025 ± 0.0010	280	6.9 ± 0.1	0.32
[^{3}H]NBI 30775	< 0.001	> 690	11 ± 0.4	<0.090
NBI 30775 [b]	< 0.001	> 690	3.6 ± 0.5	<0.27
37°C				
[^{3}H]NBI 35965	0.041 ± 0.002	17	22 ± 1	1.4
NBI 35965 [c]	0.048 ± 0.005	16	20 ± 2	3.1
[^{3}H]NBI 30775	0.0036 ± 0.0004	190	31 ± 2	0.14
NBI 30775 [c]	0.0054 ± 0.0006	130	14 ± 2.0	0.36

Kinetics of radiolabeled antagonist binding to the CRF_1 receptor was determined directly as described in Materials and Methods. See Materials and Methods for chemical name of compounds. At 22°C, k_1 was determined from the slope of a plot of $k_{1(obs)}$ versus the radioligand concentration employing six concentrations of radioligand from 1-20 nM (eq. 3, graphical data not shown for all concentrations, representative data for a single concentration shown in Fig. 2B, n=3 for [^{3}H]NBI 35965 and [^{3}H]NBI 30775). At 37°C, k_1 was determined using a single concentration of radioligand using eq. 4 (n=3 for [^{3}H]NBI 35965 and [^{3}H]NBI 30775, representative data in Fig. 2B). k_{-1} was measured by

JPET Fast Forward. Published on February 22, 2012 as DOI: 10.1124/jpet.111.188714
This article has not been copyedited and formatted. The final version may differ from this version.

adding a saturating concentration of unlabeled ligand (3 μM NBI 34041) after a 2 hr incubation of radioligand with membranes. (22°C, n=5 for [^{3}H]NBI 35965 and n=2 for [^{3}H]NBI 30775; 37°C, n=4 for [^{3}H]NBI 35965 and n=5 for [^{3}H]NBI 30775). Kinetics of unlabeled ligands was measured indirectly by competition against radiolabeled antagonists (see Fig. 3B for NBI 35965 and 3C for NBI 30775 at 37°C; graphical data at 22°C not shown). At 22°C n=2 for NBI 35965 and n=8 for NBI 30775, and at 37 °C n=19 for NBI 35965 and n=21 for NBI 30775.

[a] – K_d for radioligands determined by dividing mean k_{-1} value by mean k_1 value (eq. 7). K_i for unlabeled ligands determined as described in Table 2.

[b] – unlabeled kinetics at 22°C determined using [^{3}H]NBI 35965. The NBI 35965 pK_i was 9.50 ± 0.24, n=2. For NBI 30775, the upper K_d limit was determined by dividing the k_{-1} limit (0.001 min^{-1}) by the mean k_1 value (3.6 10^6 M^{-1}.min^{-1}).

[c] – unlabeled kinetics at 37°C determined using [^{3}H]NBI 30775, pK_i values given in Table 2, n=19-21.

JPET Fast Forward. Published on February 22, 2012 as DOI: 10.1124/jpet.111.188714
This article has not been copyedited and formatted. The final version may differ from this version.

Table 2. **Comparison of CRF_1 receptor binding kinetics and affinity for twelve lead antagonist compounds.**

Ligand	k_{-1}, min^{-1}	Dissociation $t_{1/2}$, min	k_1, $10^6 M^{-1} min^{-1}$	Kinetic pK_i [a]	Kinetic K_i [b] nM
NBI 27914	0.27 ± 0.07	2.6	9.4 ± 3	7.61 ± 0.10	25
CP-316,311	0.17 ± 0.04	4.1	13 ± 2	7.92 ± 0.09	12
NBI 46200	0.13 ± 0.002	5.3	6.2 ± 2	7.65 ± 0.15	22
DMP696	0.095 ± 0.02	7.3	7.7 ± 2	8.02 ± 0.09	9.5
pexacerfont	0.049 ± 0.001	14	2.6 ± 0.1	7.73 ± 0.03	19
NBI 35965	0.048 ± 0.005	16	20 ± 2	8.64 ± 0.05	2.3
ONO-2333Ms	0.063 ± 0.029	17	4.4 ± 2.2	7.83 ± 0.02	15
antalarmin	0.013 ± 0.002	53	3.4 ± 0.6	8.41 ± 0.06	3.9
NBI 34041	0.013 ± 0.002	53	8.3 ± 2.0	8.77 ± 0.08	1.7
DMP904	0.0072 ± 0.002	96	18 ± 1	9.42 ± 0.08	0.38
NBI 30775	0.0054 ± 0.0006	130	14 ± 2.0	9.44 ± 0.05	0.36
SSR125543A	0.0016 ± 0.0003	430	33 ± 5	10.31 ± 0.10	0.049

Kinetics of unlabeled ligands was measured indirectly by competition against radiolabeled antagonists, as described in Materials and Methods (e.g. see Fig. 2A for NBI 27914, Fig. 2B for NBI 35965, Fig. 2C for NBI 30775 and Fig. 2D for SSR125543A). See Materials and Methods for chemical name of compounds. Data are mean ± s.e.m., n=3-21. [a] – pK_i was determined from each individual experiment, involving division of k_{-1} by k_1 to determine K_i (eqn. 7), then the average and standard error of the pK_i values were calculated. [b] – K_i is the linear transformation of the mean pK_i.

JPET Fast Forward. Published on February 22, 2012 as DOI: 10.1124/jpet.111.188714
This article has not been copyedited and formatted. The final version may differ from this version.

Table 3. **Comparison of kinetic affinity with apparent affinity of lead antagonist compounds.**

Ligand	Kinetic assay vs [^{3}H]NBI 30775 @ 37 °C		Competition assay vs ^{125}I-sauvagine @ 22 °C		Competition assay vs [^{3}H]NBI 35965 @ 22 °C	
	pK_i	K_i, nM	pK_i vs	K_i, nM	pK_i	K_i, nM
NBI 27914	7.61 ± 0.10	25	8.98 ± 0.04	1.0	8.82 ± 0.13	1.5
CP-316,311	7.92 ± 0.09	12	8.71 ± 0.08	1.9	8.67 ± 0.09	2.1
NBI 46200	7.65 ± 0.15	22	8.88 ± 0.05	1.3	8.81 ± 0.11	1.5
DMP696	8.02 ± 0.09	9.5	8.65 ± 0.05	2.2	8.40 ± 0.14	4.0
pexacerfont	7.73 ± 0.03	19	8.13 ± 0.04	7.4	8.03 ± 0.01	9.4
NBI 35965	8.51 ± 0.05	3.1	8.97 ± 0.04	1.1	8.80 ± 0.07	1.6
ONO-2333Ms	7.83 ± 0.02	15	8.91 ± 0.05	1.2	8.77 ± 0.09	1.7
antalarmin	8.41 ± 0.06	3.9	8.88 ± 0.09	1.3	8.75 ± 0.21	1.8
NBI 34041	8.70 ± 0.13	2.0	8.86 ± 0.01	1.4	8.64 ± 0.15	2.3
DMP904	9.42 ± 0.08	0.38	9.24 ± 0.10	0.58	8.94 ± 0.15	1.2
NBI 30775	9.23 ± 0.08	0.59	8.58 ± 0.10	2.6	8.43 ± 0.17	3.7
SSR125543A	10.31 ± 0.10	0.049	9.53 ± 0.04	0.30	9.44 ± 0.21	0.36

See Materials and Methods for chemical name of compounds. Kinetic pK_i was measured in competition kinetics experiments performed using [^{3}H]NBI 30775 at 37 °C. pK_i was determined from each individual experiment, involving division of k_{-1} by k_1 to determine K_i (eqn. 7), then the average and standard error of the pK_i values calculated. The apparent affinity in a standard competition assay, versus the peptide antagonist ^{125}I-sauvagine, was

measured as described in Materials and Methods. The IC_{50} concentration of unlabeled ligand, measured after a 2 hr incubation at 22 °C, was converted to apparent K_i using the Cheng-Prusoff equation (^{125}I-sauvagine concentration of 63-110 pM, ^{125}I-sauvagine K_d of 20 pM). The apparent affinity was measured versus a nonpeptide antagonist, [^{3}H]NBI 35965, under the same conditions (2 hr incubation at 22 °C, [^{3}H]NBI 35965 concentration of 1.3-1.9 nM, K_d of 0.58 nM, Table 1). The pK_i was calculated from each individual experiment and the mean and s.e.m. of these p*K*i measurements given. K_i given is the linear transformation of the given mean pK_i. Single factor ANOVA indicated highly significant difference between the different measurements of affinity (***p < 0.001). A post-hoc Bonferroni post-test indicated no significant difference of apparent pK_i between [^{3}H]NBI 35965 and ^{125}I-sauvagine assays (p > 0.05 for all ligands). The same test indicated significant difference between kinetic pK_i and apparent pK_i (versus ^{125}I-sauvagine) for some ligands (*p < 0.05 for DMP904, ***p < 0.001 for NBI 27914, CP-316,311, NBI 46200, ONO-4333Ms, NBI 30775 and SSR125543A). Data are mean ± s.e.m., n=3-21.

Fig. 1

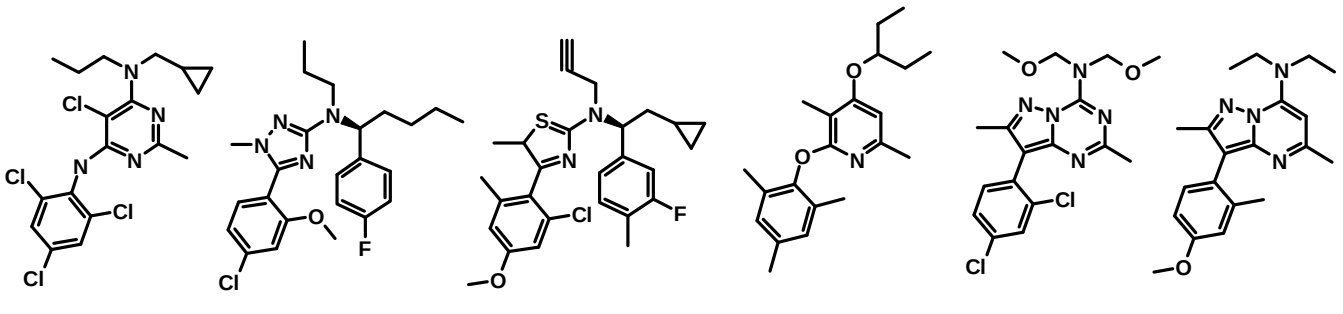

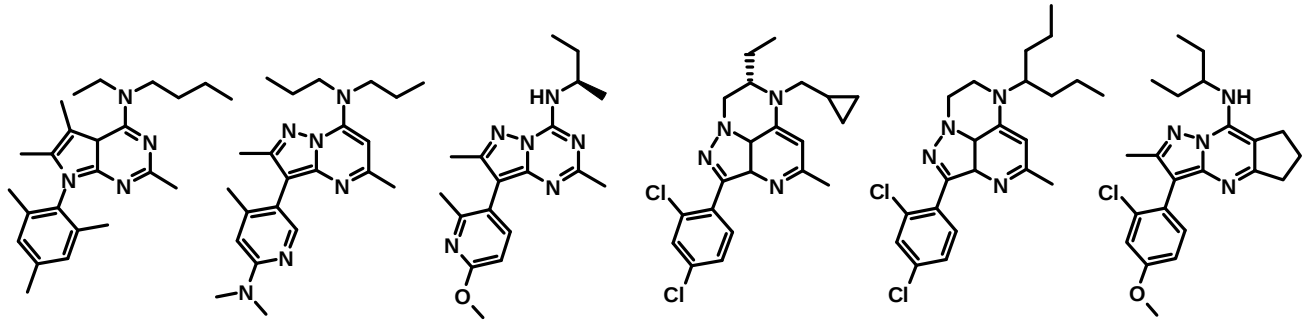

Fig. 2

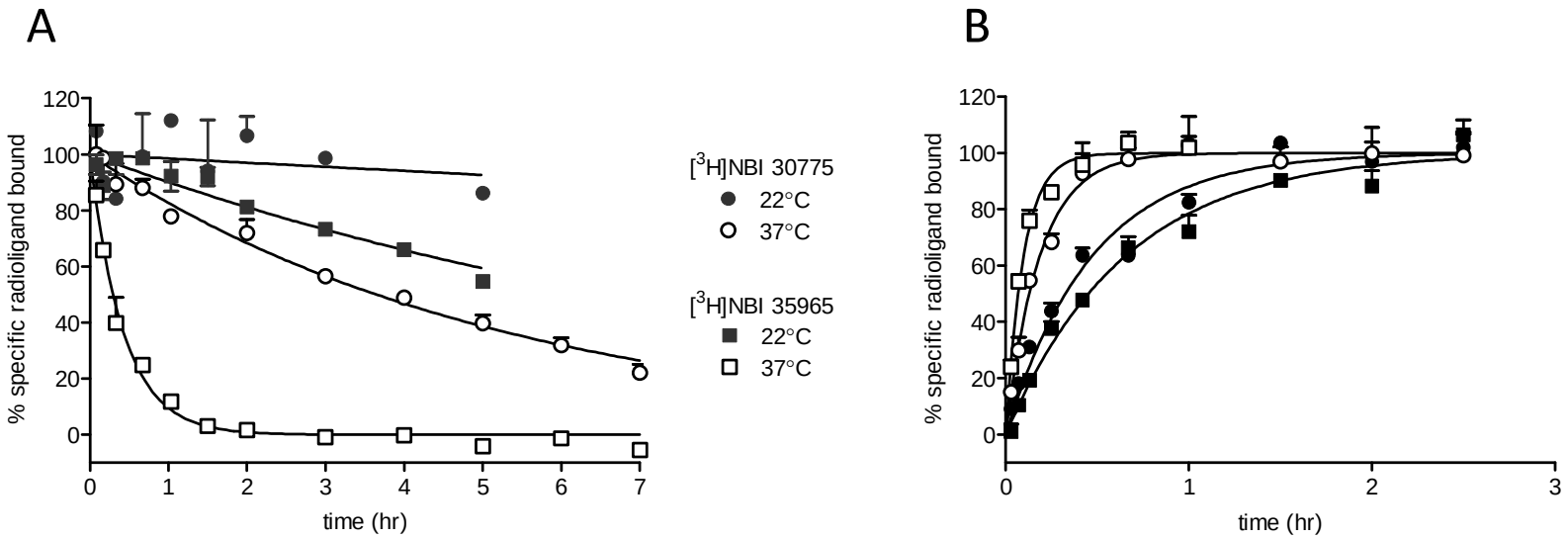

Fig. 3

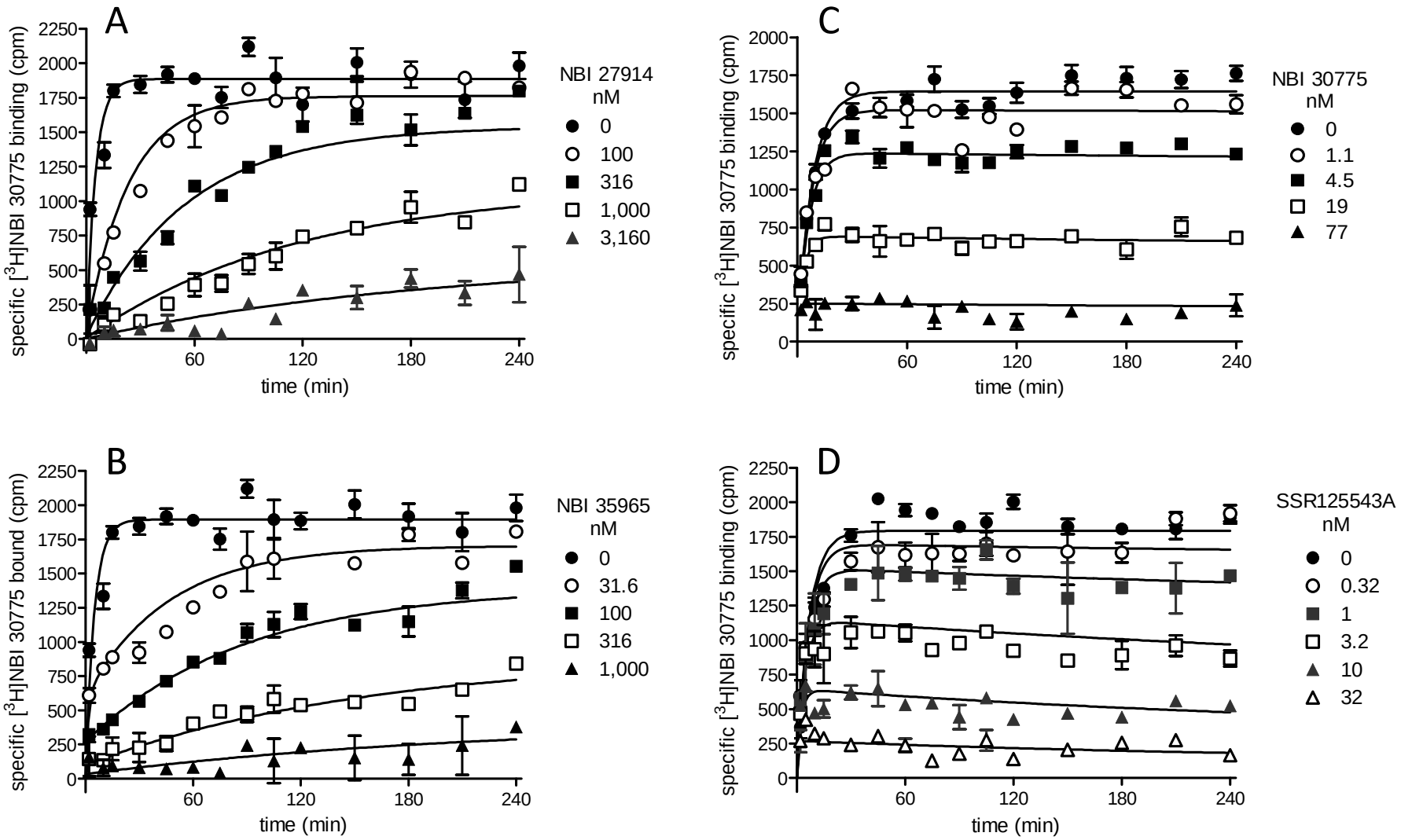

Fig. 4

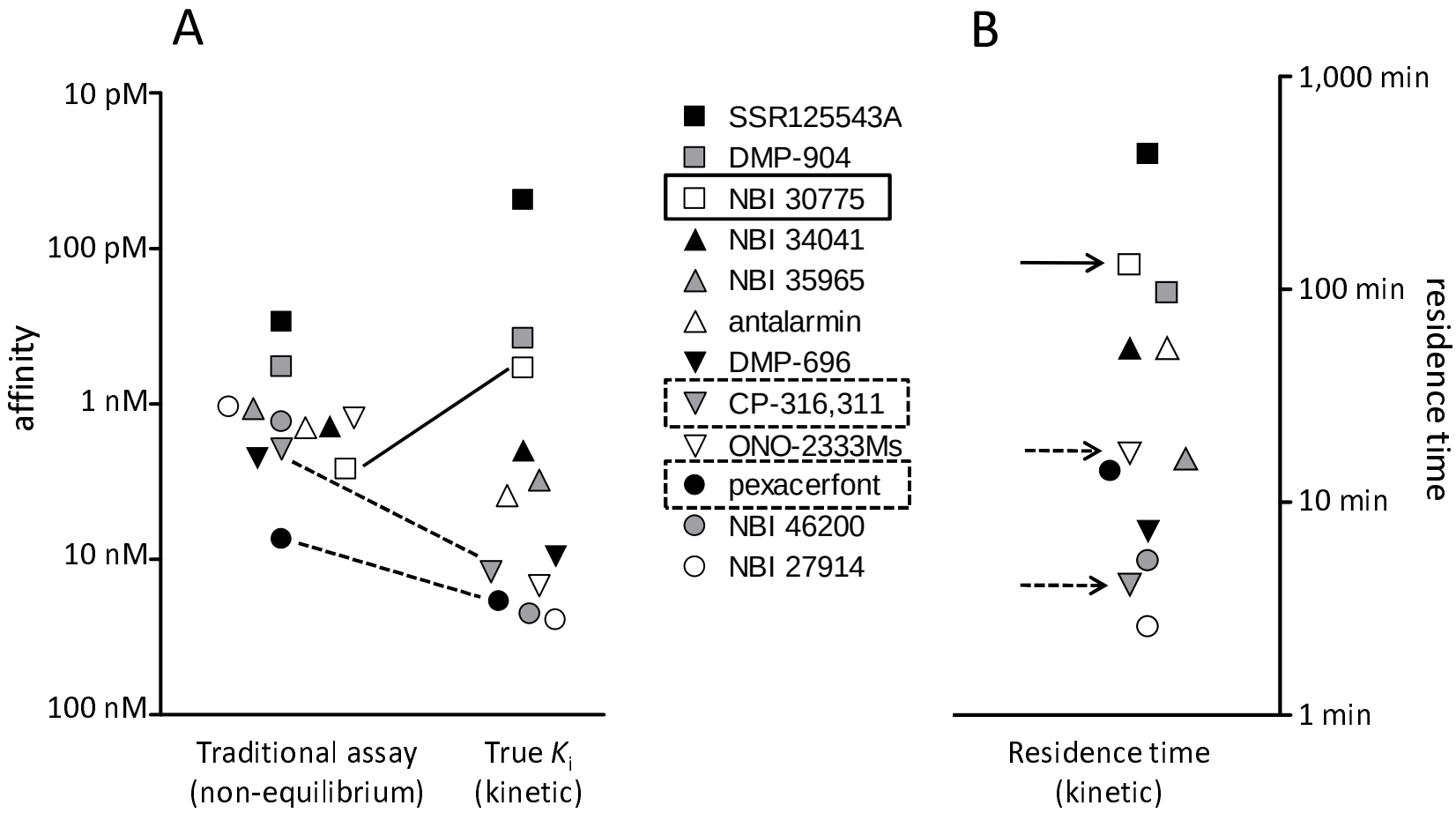

Fig. 5

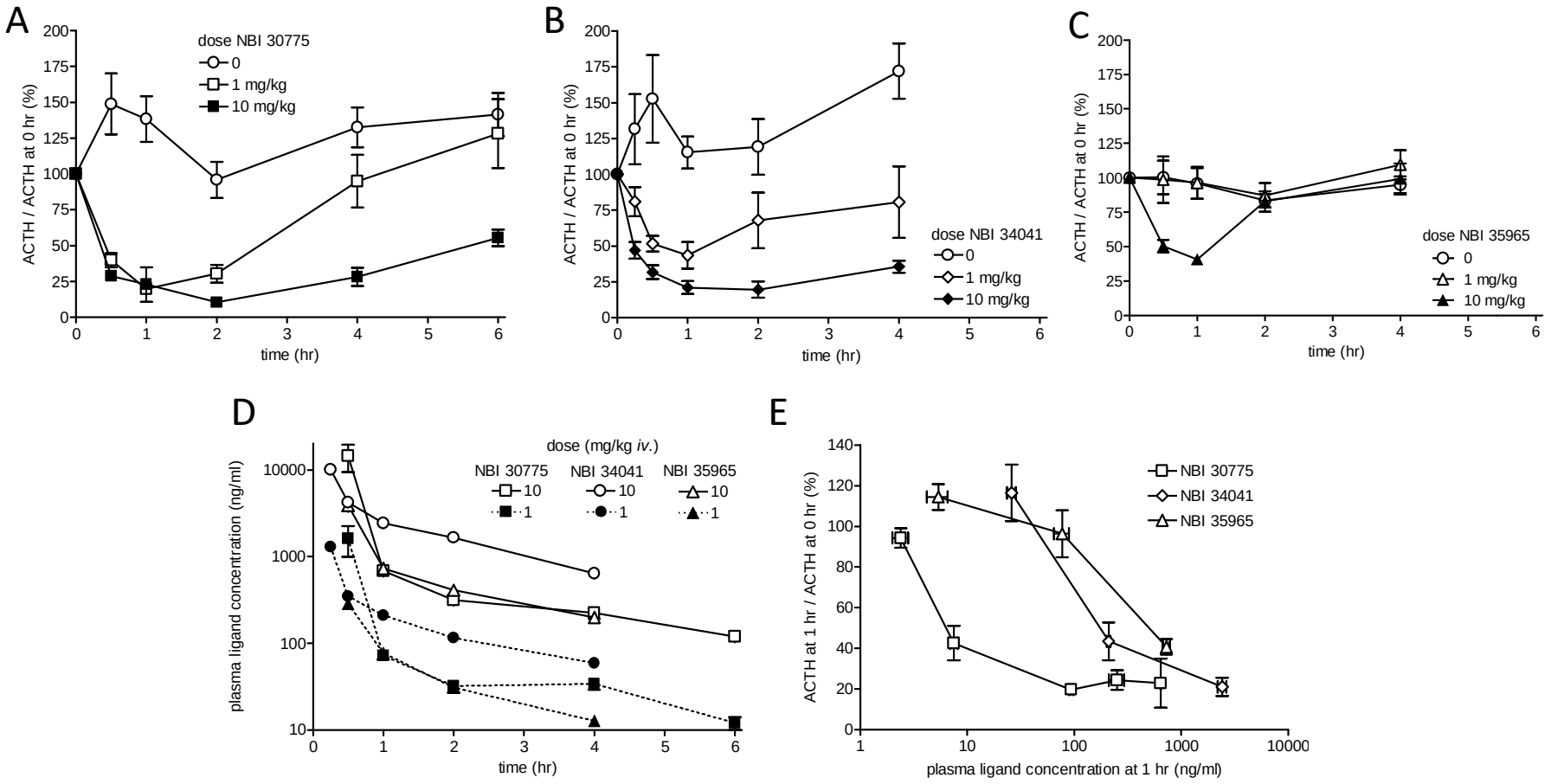

Fig. 6

R1	Ligand ID	k_{-1}, min^{-1}	k_1, 10^6 M^{-1}min^{-1}	pK_i
H	NBI 37608	0.22 ± 0.03	0.048 ± 0.021	5.25 ± 0.14
Cl	NBI 37606	0.14 ± 0.01	1.6 ± 0.3	7.05 ± 0.06

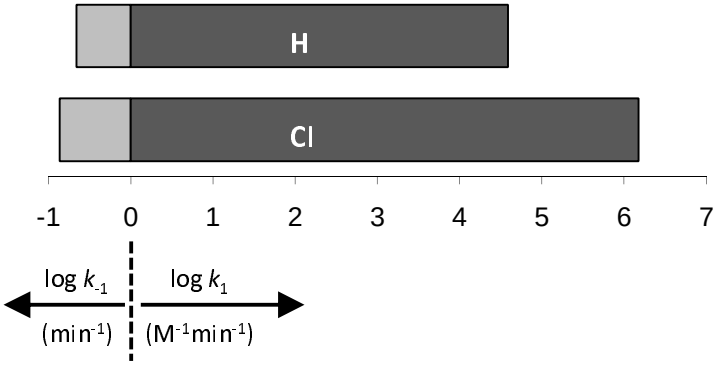

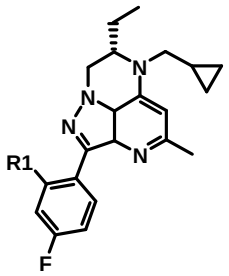

Fig. 7

R2	Ligand ID	k_{-1}, min^{-1}	k_1, 10^6 M^{-1}min^{-1}	pK_i
H	NBI 49721	0.22 ± 0.09	0.12 ± 0.05	5.74 ± 0.01
CH_3	NBI 34041	0.013 ± 0.002	8.3 ± 2.0	8.77 ± 0.08

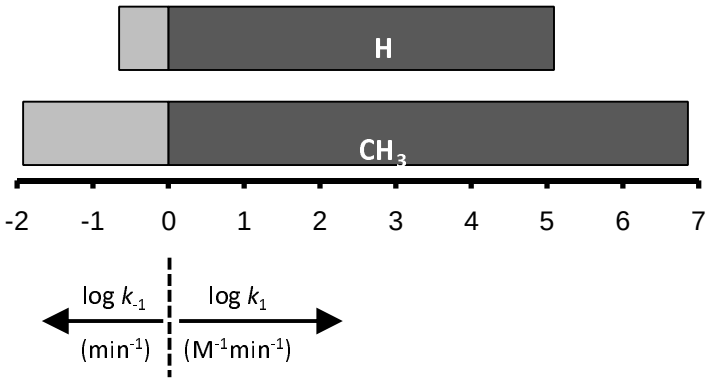

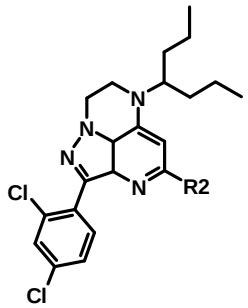

Fig. 8

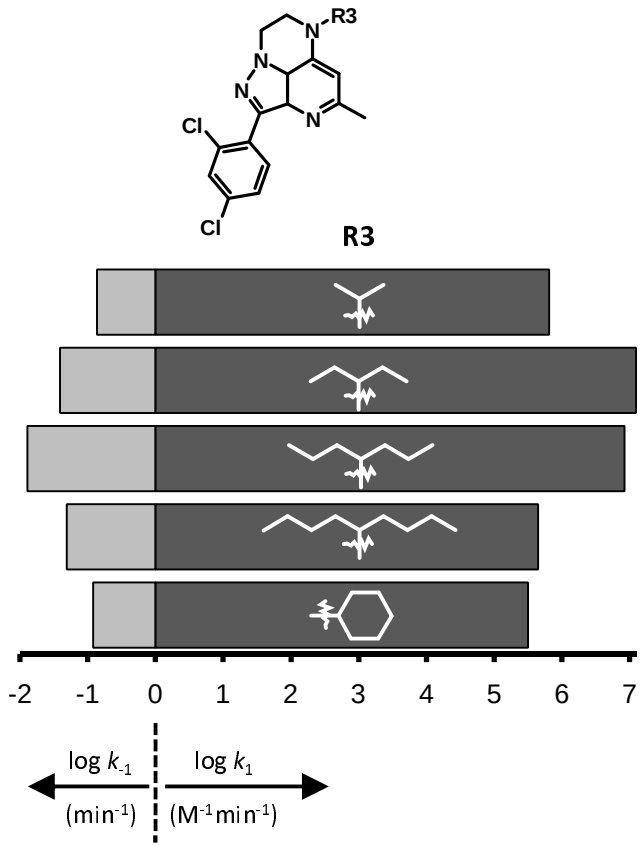

k_{-1}, min^{-1}	k_1, 10^6 $M^{-1}min^{-1}$	pK_i	Ligand ID
0.16 ± 0.07	0.68 ± 0.08	6.70 ± 0.13	NBI 78194
0.039 ± 0.004	12 ± 1	8.50 ± 0.03	NBI 34417
0.013 ± 0.003	8.3 ± 2.0	8.77 ± 0.08	NBI 34041
0.049 ± 0.008	0.45 ± 0.04	6.97 ± 0.10	NBI 34416
0.12 ± 0.03	0.32 ± 0.01	6.44 ± 0.12	NBI 34802

Fig. 9